



# Graphitization of Neoproterozoic sedimentary marbles in The Aird, Scottish Highlands

Eleanor A. Heptinstall<sup>1\*</sup>, John Parnell<sup>1</sup>, Andrea Schito<sup>1,2</sup>, Adrian J. Boyce<sup>3</sup>, Joseph G. T. Armstrong<sup>1</sup> and David Muirhead<sup>1</sup>

<sup>1</sup> School of Geosciences, University of Aberdeen, Meston Building, Kings College, Aberdeen AB24 3UE, UK

<sup>2</sup> Faculty of Earth Sciences, University of Barcelona, Martí i Franquès, s/n, Les Corts, Barcelona 08028, Spain

<sup>3</sup> Scottish Universities Environmental Research Centre, Rankine Avenue, Glasgow G75 0QF, UK

EAH, 0000-0002-6890-2399

\* Correspondence: [e.heptinstall.18@abdn.ac.uk](mailto:e.heptinstall.18@abdn.ac.uk)

**Abstract:** Graphite occurs in Neoproterozoic (probable Loch Ness Supergroup) marbles of The Aird, in the Northern Highland Terrane, Scotland. The graphite occurs particularly in association with phlogopite mica, and also with other micas and Mg-chlorite. Although the graphite–phlogopite association is recorded widely elsewhere in mantle-derived rocks, our data suggest graphite at The Aird does not have a mantle origin. The carbon isotopic composition of the graphite ( $\delta^{13}\text{C}$ :  $-1.6$  to  $0.4\%$ ) indicates that graphitization occurred from a  $\text{CO}_2$ -rich fluid associated with decarbonation or devolatilization reactions of a carbonate–silicate protolith. Graphite–phlogopite-bearing marbles in The Aird underwent extensive brecciation and hematite deposition that preceded carbon-rich, mantle-derived (carbonatite) fluids. Pyrite in veins within The Aird marble has a sulfur isotope composition depleted in  $^{34}\text{S}$  ( $-16.6$  to  $-15.5\%$ ), suggesting a biogenic origin. Elsewhere in The Aird and in surrounding fenitized rocks,  $^{34}\text{S}$ -enriched pyrite has sulfur isotope compositions between  $6.1$  and  $7.7\%$ , outside the sulfur isotopic composition range of most carbonatite-hosted pyrite, suggesting that pyrite veining is likely to have been influenced by crustal fluid–rock interactions. The observations show that if the protolith has a carbonate–silicate composition, a graphite–phlogopite association can form without the need for mantle-derived fluids.

**Thematic collection:** This article is part of the Early Career Research collection available at: <https://www.lyellcollection.org/topic/collections/early-career-research>

Received 25 July 2023; revised 21 April 2024; accepted 7 May 2024

Graphite occurs in metamorphic and igneous rocks, where it mineralizes by solid-state organic matter recrystallization or nucleation and crystal growth from a carbon-rich fluid. Carbon-derived fluids are usually derived from a carbonate protolith or the intrusion of a magmatic component. The decarbonation or devolatilization of carbonate rocks, fixation of C–O–H fluids to nucleation sites and crystal growth mechanisms strongly influence crystallography, graphite texture (i.e. size, shape and assemblage arrangement) and morphology (i.e. atomic geometric structure, overgrowth or twinning characteristics) (e.g. Jaszczak 1997; Satish-Kumar *et al.* 2011; Luque *et al.* 2012; Moro *et al.* 2017). These constraints on graphite mineralization in association with micaceous or sulfide minerals, together with thermometry constraints (Peck *et al.* 2006; Satish-Kumar *et al.* 2011) and carbon isotopic compositions (Satish-Kumar and Wada 2000; Luque *et al.* 2012), are important to the interpretation of graphitization histories.

The Aird is a geographical and distinctive geological region hosting marble, regions of fenitization and intrusive pegmatite rocks in the Scottish Highlands (Fig. 1), bound to the north by the Beaully Firth and the south by fenitized Abriachan granites and psammities, up to 12 km to the west and SW of Inverness. Graphite–phlogopite mixtures occur in metamorphosed limestones in The Aird region of Scotland that are geologically distinct from successions of Loch Ness Supergroup metasedimentary rocks elsewhere in northern

Scotland. Graphitic metamorphosed limestones occur with calcite-rich igneous rocks in The Aird, a combination that is rare in the UK. The origin of graphite is poorly constrained due to limited geological attention and previous assumptions that graphite was rare within the Wester Ross and Loch Ness supergroups. The proximity of The Aird to the Great Glen Fault also has received limited research with respect to shear zone-derived modification of graphitic host rocks by brecciation, veining and shearing. In this paper, we report a graphite–phlogopite association in the Neoproterozoic marbles of The Aird and discuss its formation and post-orogenic modification.

Graphite-bearing marble occurrences are investigated in Moniak Burn, Rebeg, Kirkton and Blairnahenachrie in The Aird, a limited region NW of the Great Glen Fault, and are compared to three other marble occurrences in the region, at Glen Urquhart, Scardroy and Rosemarkie (Fig. 1). Marble occurrences at Scardroy and Rosemarkie are attributed to Paleoproterozoic inliers tectonically emplaced within Loch Ness Supergroup rocks (Sutton and Watson 1951; Rathbone and Harris 1980; Strachan *et al.* 2010). The Scardroy locality includes layers of graphitic schist and graphite nodules in marble, associated with 2.7 Ga gneisses (Rock *et al.* 1987; Parnell *et al.* 2021). Rosemarkie hosts carbonates with late Caledonian pegmatite intrusions, carbonatitic veining and breccia veins that are also present in nearby Glenfinnan Group metasedimentary rocks (Garson *et al.* 1984). Marble

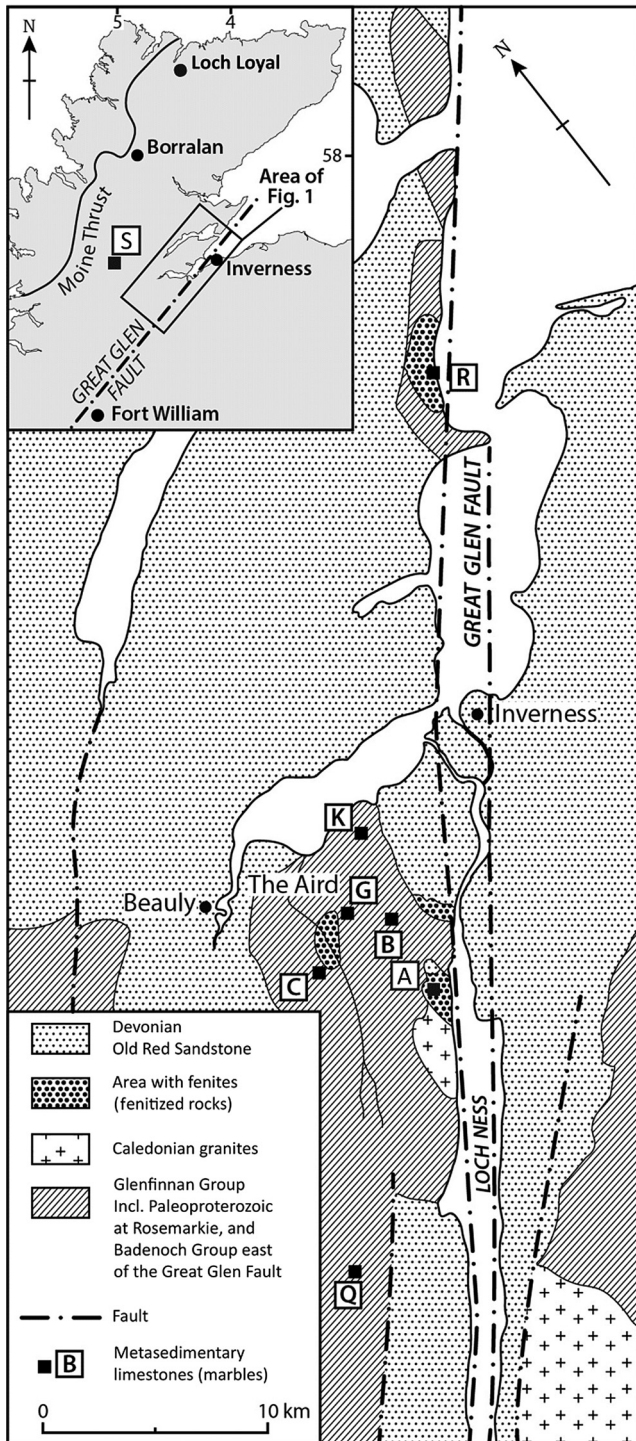


**Fig. 1.** Geological map of the region along the Great Glen Fault in the vicinity of Inverness, showing occurrences of metasedimentary limestone (marble) and regions of fenitization. Limestone occurrences: A, Abriachan; B, Blairnahenachrie; C, South Clunes; G, Rebeg; K, Kirkton; Q, Glen Urquhart; R, Rosemarkie. The Paleoproterozoic Scardroy Inlier (Scardroy), Loch Borralan Alkaline Complex (Loch Borralan) and Loch Loyal Syenite Complex (Loch Loyal) are also shown for reference. Source: adapted from *Garson et al. (1984)*.

at Glen Urquhart, the closest to The Aird, was large enough to be quarried, as at The Aird. It has been variably compared with Lewisian, Loch Ness Supergroup and Dalradian rocks but distinctions in trace element compositions saw it allocated to a distinct Neoproterozoic division (*Rock et al. 1986a*). The Glen Urquhart albite-bearing marble is associated with kyanite-graphite mica-schist (*Brook and*

*Rock 1983; Garson et al. 1984*). More recently, a comparison of detrital zircon age dates with those from undoubted Loch Ness Supergroup strata has reaffirmed a Neoproterozoic age for the Glen Urquhart rocks but with some ambiguity about whether it belongs to the Loch Eil Group (*Cawood et al. 2004*), the Glenfinnan Group (*Cutts et al. 2010*), or possibly a distinct succession (*Cawood et al. 2015*).

Graphite-bearing rocks were recorded in *Rock et al. (1984)* as limestone and pelites, the former having previously been considered very rare in the Loch Ness Supergroup, whilst carbonatite veins were described in The Aird by *Garson et al. (1984)*. The occurrence of graphite is unusual in magmatic carbonatites (*Doroshkevitch et al. 2007*) but the inference of carbonatite activity near The Aird raises the possibility that The Aird graphite is derived from carbonatitic fluids. This study investigates metamorphosed limestones (hereafter referred to as marbles) that are enriched in graphite, and the context of the graphite, by assessing:

- (i) If the carbon isotopic composition of the graphite can constrain the origin of the carbon in the protolith carbonate.
- (ii) If thermometry findings from Raman spectroscopy and fluid-inclusion analysis suggest that graphite and its associative minerals were mineralized during regional metamorphism (i.e. it was mineralized as graphite) or was associated with later carbonatite-related fluids.
- (iii) If the sulfur isotopic composition of accompanying sulfide precipitation may corroborate a sedimentary or mantle carbon origin for the graphite.
- (iv) A paragenesis for the graphite and other mineral phases in the marble during the Grampian I/II and Scandian orogenies
- (v) The post-Grampian I/II modification of graphite and marble host rocks, and how these compare to previous observations of graphitic host rocks.

## Fluid-derived graphitization

### Carbonate decarbonation and devolatilization

The controls of carbon removal from a protolith carbonate are dependent on oxidation- or reduction-related carbonate mineral destabilization, and the mixing of C–O–H fluids during amphibolite- to granulite-facies metamorphism associated with slab descent in subduction zones (*Ague 2000; Galvez et al. 2013; Ague and Nicolescu 2014*), orogenic episodes (*Rumble et al. 1986; Evans et al. 2002*) or igneous-intrusive shearing (*Satish-Kumar 2005*). Carbonate-derived graphitization can occur through two processes: decarbonation and devolatilization. The former varies from carbonate reduction  $\pm$  mixing with mantle-derived fluids (*Rumble et al. 1986*) that yields isotopically heavy graphite (*Satish-Kumar et al. 2011; Luque et al. 2012; Parnell et al. 2021*); and the latter through mixing of carbon-saturated aqueous fluids derived from carbonate and sedimentary protoliths, which usually yields lighter carbon isotopic compositions of graphite (*Evans et al. 2002; Satish-Kumar 2005; Luque et al. 2012*). Decarbonation-related graphitization in the absence of igneous fluids usually occurs through carbonate reduction and subsequent reactions of a carbon-

saturated C–O–H fluid (Galvez *et al.* 2013) between authigenic minerals, calcite and/or dolomite with quartz or other silicates (Luque *et al.* 2012). Devolatilization-related graphitization occurs from the oxidation and dissolution of carbonate minerals (i.e. calcite and dolomite), leading to volatile reactions with low oxygen fugacity fluids derived from organic carbon and/or silicate minerals (e.g. micas, garnets and amphiboles) in metasedimentary rocks, usually within interlayered or conformable sequences (e.g. Rumble *et al.* 1986; Evans *et al.* 2002; Satish-Kumar 2005).

### Graphite–phlogopite associations

Graphite can occur in a range of geological environments, from the contact or regional metamorphism of kerogen in carbonaceous sediments (Wada *et al.* 1994; Wright *et al.* 2012) to fluid-phase deposition from carbonate or igneous fluids (Ferraris *et al.* 2004; Luque *et al.* 2012; Galvez *et al.* 2013). The mineralization of graphite from a fluid phase can be influenced by minerals which have layer-silicate surface properties at the nanoscale that enhance admixture with carbon (Moro *et al.* 2017). Phlogopite mica is one such mineral, occurring commonly within ultramafic and carbon-rich magmas, as well as in marbles. The association of phlogopite with reduced carbon in marbles (Peck *et al.* 2006) can make it challenging to distinguish them from the same association in mantle-derived carbonatitic intrusions (Le Bas *et al.* 2002; Ferraris *et al.* 2004; Humphreys-Williams and Zahirovic 2021). Graphite–phlogopite mixtures in mantle-derived ultramafic and carbonatite rocks suggest that phlogopite can act as a preferred template for carbon, and have been interpreted to indicate a mantle reservoir of carbon (Ferraris *et al.* 2004; Rajesh *et al.* 2009; Ashchepkov *et al.* 2015; Kelemen and Manning 2015; Galvez *et al.* 2020; Humphreys-Williams and Zahirovic 2021). Graphite–phlogopite admixtures have been found in mantle-origin Iherzolite (Ferraris *et al.* 2004), peridotite xenolith mixtures (Kaesler *et al.* 2007), kimberlite pipes (Kostrovitsky *et al.* 2001), carbonatitic fluids described in peridotite (Naemura *et al.* 2009) and carbon–phlogopite assemblages in the mantle wedge of subduction zones (Kelemen and Manning 2015).

Graphite–phlogopite assemblages have been known to occur in metamorphosed carbonate–metasedimentary rocks. Some of these graphite–phlogopite occurrences occur in gemstone marbles, notably the ruby-bearing marble–sillimanite gneiss belts from Afghanistan to China (Yang *et al.* 2019) and Vietnam (Hauzenberger *et al.* 2005), ruby/corundum-bearing marble/calc-silicates in British Columbia (Dzikowski *et al.* 2014) and sapphire/corundum-bearing marble/calc-silicate on Baffin Island (Belley *et al.* 2017). Graphite–phlogopite assemblages are widely documented in mixed carbonate–silicate deposits, including the Ampandrandava metacarbonate interlayered with graphitic-sillimanite schist in Sri Lanka (Satish-Kumar *et al.* 2021) and granulite-facies marble assemblages in the Skallen region of East Antarctica (Satish-Kumar and Wada 2000). An example of graphite-bearing marbles comparable with those in The Aird forms part of a suite of granulite-facies Mesoproterozoic marbles in the New Jersey Highlands (Peck *et al.* 2006). Graphite–phlogopite nodules occur in pyritic, calcite marble

in Lime Quest, New Jersey, where nodules up to 1 cm in size were identified and extracted by Jaszczak (1997). Graphite–phlogopite nodules shown in Jaszczak (1997) highlighted varied graphite–phlogopite crystal morphologies of basal pinacoid faces of millimetre-scale tabular ± overgrowth crystals, hexagonal crystals and spherical crystal clusters of graphite minerals. Graphite also occurs nearby in marble at Ogdensburg, New Jersey (Palache 1941; Jaszczak 1994). Palache (1941) and Jaszczak (1997) identified graphite–phlogopite with graphite overgrowths, and spherical graphite attached to phlogopite crystal surfaces.

Graphite–phlogopite assemblages, their crystal atomic structure and crystal composition were analysed using different forms of scanning electron microscopy (SEM), including electron dispersive spectroscopy (Jaszczak 1997), X-ray diffraction (XRD) using field emission scanning electron microscopy (FE-SEM) (Satish-Kumar *et al.* 2011) or electron microprobe analysis (Ferraris *et al.* 2004). Hydrocarbon–phlogopite-bearing fluid inclusions were also imaged using confocal microscopy dimensions at the nanometre to micrometre scale (Moro *et al.* 2017). Carbon isotopic compositions, SEM microphotography and Raman spectroscopy of nodular graphite–phlogopite constrained temperature-dependent calcite–graphite geothermometry, graphite morphology and crystallinity in studies by Satish-Kumar *et al.* (2011), who distinguished two distinct graphite populations: the highly crystalline, platy graphite, mineralized in isotopic equilibrium with carbonate-derived CO<sub>2</sub> fluids; and phlogopite-enclosed disordered graphite with distinctively lower δ<sup>13</sup>C compositions. Graphite–phlogopite ordering is discussed in Ferraris *et al.* (2004), who also utilized Raman spectrometry alongside high-resolution transmission electron microscopy (HRTEM) to indicate co-precipitation and topotactic intergrowth of laminae graphite and phlogopite, connected by layers of weak van der Waals bonds.

## Geological setting

### Regional geology

The Lewisian Foreland Terrane, Northern Highlands Terrane and Grampian Terrane are three distinct geological regions in the Scottish Highlands that comprise Proterozoic successions. The Northern Highlands Terrane comprises poly-metamorphosed, late Mesoproterozoic–Neoproterozoic (1000–870 Ma) fluvial–marine metasandstone and metapelite successions cut by Caledonian intrusive rocks (Strachan *et al.* 2010; Cawood *et al.* 2015; Krabbendam *et al.* 2022). The Moine Thrust (Fig. 1) separates the Northern Highlands Terrane from Archean–Paleoproterozoic gneisses, Neoproterozoic Torridon sandstones and later Paleozoic rocks in the Lewisian Foreland Terrane. The southern boundary of the Northern Highlands Terrane is the Great Glen Fault, which separates it from the Neoproterozoic–Lower Paleozoic metasediments and Caledonian intrusive rocks in the Grampian Terrane (Chew and Strachan 2014; Krabbendam *et al.* 2022).

The Wester Ross Supergroup in the Northern Highlands Terrane is confined to the Moine Nappe between the Caledonian or older Moine and Sgurr Beag thrusts, and is

comprised entirely of the Morar Group of metasedimentary lithologies that record Renlandian prograde amphibolite-facies metamorphism at *c.* 950–940 Ma (Bird *et al.* 2018). The structurally overlying Loch Ness Supergroup (Krabbendam *et al.* 2022) records the Sgurr Beag Nappe-hosted Glenfinnan and Loch Eil groups, that were deposited prior to the 840–725 Ma Knoydartian Orogeny (Mako *et al.* 2021; Krabbendam *et al.* 2022). Metasedimentary rocks of The Aird and Glen Urquhart are positioned in the hinterland of the Sgurr Beag Nappe. Mako *et al.* (2021) described polymetamorphosed accessory phases in Glen Urquhart, and the isotopic resetting of monazite and xenotime in 750 Ma quartz-feldspathic metasedimentary rocks by later reprecipitation at 600 and 425 Ma.

The Northern Highlands Terrane hosts inliers of Archean–Paleoproterozoic basement, comprising eclogites (Bird *et al.* 2023), mafic–intermediate orthogneisses and reworked amphibolite-facies 2.5–1.8 Ga supracrustal rocks (Strachan *et al.* 2020b); the latter described by Rock *et al.* (1987) as comprising amphibolite–granulite-facies silicic gneisses, amphibolites, calc-silicates and marbles. The Caledonian Orogeny reworked numerous stratigraphic successions in the Northern Highlands Terrane through greenschist–amphibolite-facies regional metamorphism and tight folding during the 470–460 Ma Grampian event (i.e. Grampian I) (Strachan *et al.* 2010; Mako *et al.* 2021; Krabbendam *et al.* 2022). A further compressional event in the west and far north of the Northern Highlands Terrane, termed Grampian II, occurred at *c.* 450 Ma (Bird *et al.* 2013), followed by plutonism at Glen Dessary (Goodenough *et al.* 2011; Milne *et al.* 2023). Orogenesis related to Grampian II in the Glenfinnan Group (Bird *et al.* 2013) and fault-bound plutonism (Milne *et al.* 2023) is documented to the west of the Great Glen Shear Zone. However, this remains underexplored in Glenfinnan Group rocks to the north of the Great Glen Shear Zone (Bird *et al.* 2013). The Scandian event between *c.* 437 and *c.* 415 Ma (Oliver *et al.* 2008; Strachan *et al.* 2010) led to widespread upright refolding of earlier structures, and from *c.* 432 Ma onwards was accompanied by widespread intrusion of granitoids (Milne *et al.* 2023). Some of these bodies in Glen Scaddle and the Assynt Alkaline Complex record Scandian ductile deformation (Strachan and Evans 2008; Goodenough *et al.* 2011), whilst others are unaffected (e.g. Cluanie: Milne *et al.* 2023).

Regional transpression throughout northern Scotland and granite emplacement through transpressive and transtensive faults (i.e. Newer Granites) occurred following the Scandian Orogeny at *c.* 430 Ma (Dewey and Strachan 2003; Strachan *et al.* 2010, 2020a; MacRae *et al.* 2023; Milne *et al.* 2023). The intrusion of the Abriachan Granite has recently been constrained to  $420.1 \pm 3.4$  Ma (MacRae *et al.* 2023), placing a further upper limit on widespread regional fenitization and alkaline carbonatitic mineralization (Deans *et al.* 1971; Garson *et al.* 1984; Heptinstall *et al.* 2023). Sinistral displacement on the Great Glen Fault system dates back to at least *c.* 428 Ma where it is recorded in shear zones associated with the emplacement of Clunes tonalite (Stewart *et al.* 2001). Sinistral motion is considered to have persisted until *c.* 400 Ma, when syntectonic granitoid emplacement is recorded at Rosemarkie (Mendum and Noble 2010). Within the overall context of sinistral fault motion, there was a

switch from regional transpression to transtension at the end of the Scandian Orogeny at *c.* 415 Ma (Dewey and Strachan 2003; Strachan *et al.* 2020a). Late Caledonian successor basins were infilled in the Devonian by Old Red Sandstone successions to the north and the east of the Northern Highland Terrane (Parnell 1985; Elmore *et al.* 2006). The Great Glen Fault experienced multiple phases of largely dextral reactivation during basin inversion and extensional events, including during the later Devonian, Carboniferous–Permian, Jurassic–Cretaceous and early Cenozoic (Underhill and Brodie 1993; Le Breton *et al.* 2013; Dichiarante *et al.* 2016, 2020; Tamas *et al.* 2023).

### The Aird local geology

The Aird marble was quarried at four main sites in the Glenfinnan Group: at Rebeg, South Clunes, Blairnahenachrie and Kirkton (Jolly and Cameron 1880; Wallace 1885, 1887; Peach *et al.* 1913; Home and Hinxman 1914). Rock *et al.* (1984) described the South Clunes, Rebeg and Kirkton quarries as consisting predominantly of marble, which is interlayered with pelitic schists at Kirkton. The marbles are known to be cross-cut by pegmatites, and exhibit brecciated fabric, hematite veins and fenitization (metasomatic alteration by alkaline fluids). Fenitization was described by Garson *et al.* (1984), particularly veins bearing the blue amphibole magnesioriebeckite (previously termed crocidolite because of the colour). Fenitization has been interpreted as an alteration of country rock by alkaline and carbonatite fluids (Elliott *et al.* 2018) in the region of the Great Glen Fault (Deans *et al.* 1971; Garson *et al.* 1984). Marble in The Aird is today exposed as isolated outcrops and fluvial boulders in the Moniak Burn derived from the quarries at Rebeg and South Clunes.

Limestones are poorly documented in the Wester Ross Supergroup and Loch Ness Supergroup successions of the former Moine Supergroup (Rock *et al.* 1986b). Although they are barely exposed now, old records indicate that the marbles of The Aird were formerly more widely reported and mined. The New Statistical Account for Scotland (Fraser 1845) records ‘numerous beds of primary granular limestone’ (p. 492), and Wallace (1885) reported that quarrying was ‘very successfully carried on for a good many years’, ‘kilns ... on an unusually large scale for this district’ and ‘great quantities were shipped, and for this purpose a canal was cut by the late proprietor’ (p. 170). These descriptions do not accord with the assumed lack of limestone in the Neoproterozoic.

Marbles in The Aird stratigraphically overlie other metasedimentary rocks of Neoproterozoic age, laid down around *c.* 870 Ma, and may have undergone prior metamorphism in Proterozoic times. However, the influence of the Caledonian Orogeny in The Aird is indicated by zircon hosted in intrusive pegmatite (Cutts *et al.* 2010), which has yielded a U–Pb age of  $463 \pm 4$  Ma. This age is considered to correspond to a time of folding and fabric development in the Loch Ness Supergroup during the Grampian Orogeny. Monazite hosted in graphite–kyanite schist at Glen Urquhart gave a similar U–Pb date of  $473 \pm 2$  Ma (Mako *et al.* 2021). Carbonatitic veining in the Great Glen region was previously documented by Garson *et al.* (1984) and has

recently been investigated for trace metal-bearing minerals in The Aird carbonatitic veins (Heptinstall *et al.* 2023). The carbonatite veins described in The Aird may have been intruded coeval with the *c.* 429–425 Ma emplacement of the ‘Newer Granites’ (Rogers and Dunning 1991; Milne *et al.* 2023) and mafic–peralkaline Moine Thrust granitoids (Goodenough *et al.* 2011; Walters *et al.* 2013), the emplacement of the *c.* 420 Ma Abriachan alkaline granite (MacRae *et al.* 2023), or later lamprophyre dyke swarms that were intruded up to *c.* 410 Ma elsewhere in the Great Glen Shear Zone (Searle 2022). This study will assess carbon and sulfur isotopic compositions of graphite and accessory sulfide minerals to investigate the paragenesis and post-Grampian I/II modification of graphite–phlogopite minerals during the Caledonian Orogeny.

## Methodology

Graphite, phlogopite and pyrite-bearing samples in The Aird were collected by the authors, based in the Geology and Geophysics Department at the University of Aberdeen, from outcrops at the Kirkton and Rebeg quarries, an exposure at Blairnahenachrie, and from a stream section cutting marbles in Moniack Burn (Fig. 1). Key specimens highlight graphite mineralization and Caledonian Orogen paragenesis (Fig. 2).

The Moniack Burn stream section is adjacent to outcrops of highly weathered black marble with cross-cutting carbonatitic veining at Rebeg Quarry. A single *c.* 3–4 kg block of graphitic marble was sampled from the poorly exposed bedrock at Glen Urquhart. We do recognize, however, that a single sample at Blairnahenachrie and Glen Urquhart can have representative limitations.

High-resolution image and compositional analyses were performed at the University of Aberdeen ACEMAC Facility using a Zeiss Gemini field emission gun scanning electron microscope (FEG-SEM) on polished blocks of the marble. Samples were carbon coated and analysed at 20 kV, with a working distance of 10.5 mm. Marble samples were examined through electron dispersive spectrometry (EDS) of graphite-bearing nodules (Fig. 3), and graphite entrained within pyrite veins (Fig. 4) was analysed using Oxford Instruments EDS X-ray analysis to ascertain compositional data on the phlogopite minerals, which assumes 22 oxygen equivalents (Table 1). The standards used were a mixture of natural minerals, metal oxides and pure metals, with calibrated by per the factory specification. Stoichiometry was determined by fixed oxygen contents of specific minerals, which has a compositional error of *c.* 0.01 wt%, with atomic unit calculations assuming 11 oxygens per formula in order to be comparable to the phlogopite empirical formula.

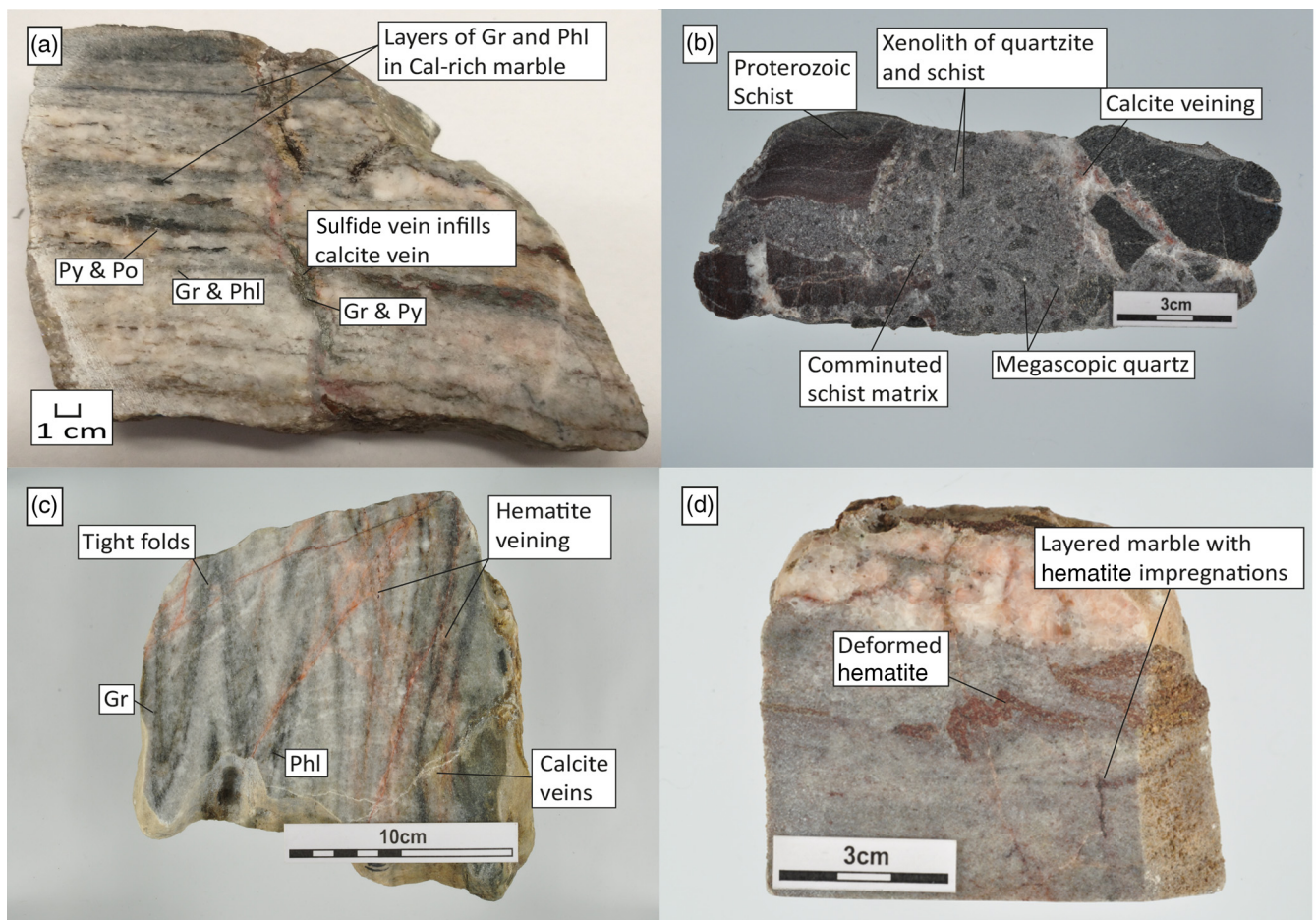


**Fig. 2.** The Aird specimen photographic images. (a) Layered marble enriched in graphite, phlogopite and pyrite, cut by a calcite vein and a later parallel sulfide vein. (b) Hydraulic breccia vein through schist metasediment, comprising comminuted country rock and euhedral megascopic quartz. (c) Tightly folded marble with folding defined by dark graphite-bearing layers, cross-cut by undeformed hematite veins. (d) Layered marble cross-cut by hematite veins and accumulations, some of which underwent later deformation. Labels: Gr, graphite; Phl, phlogopite; Po, pyrroite; Py, pyrite.

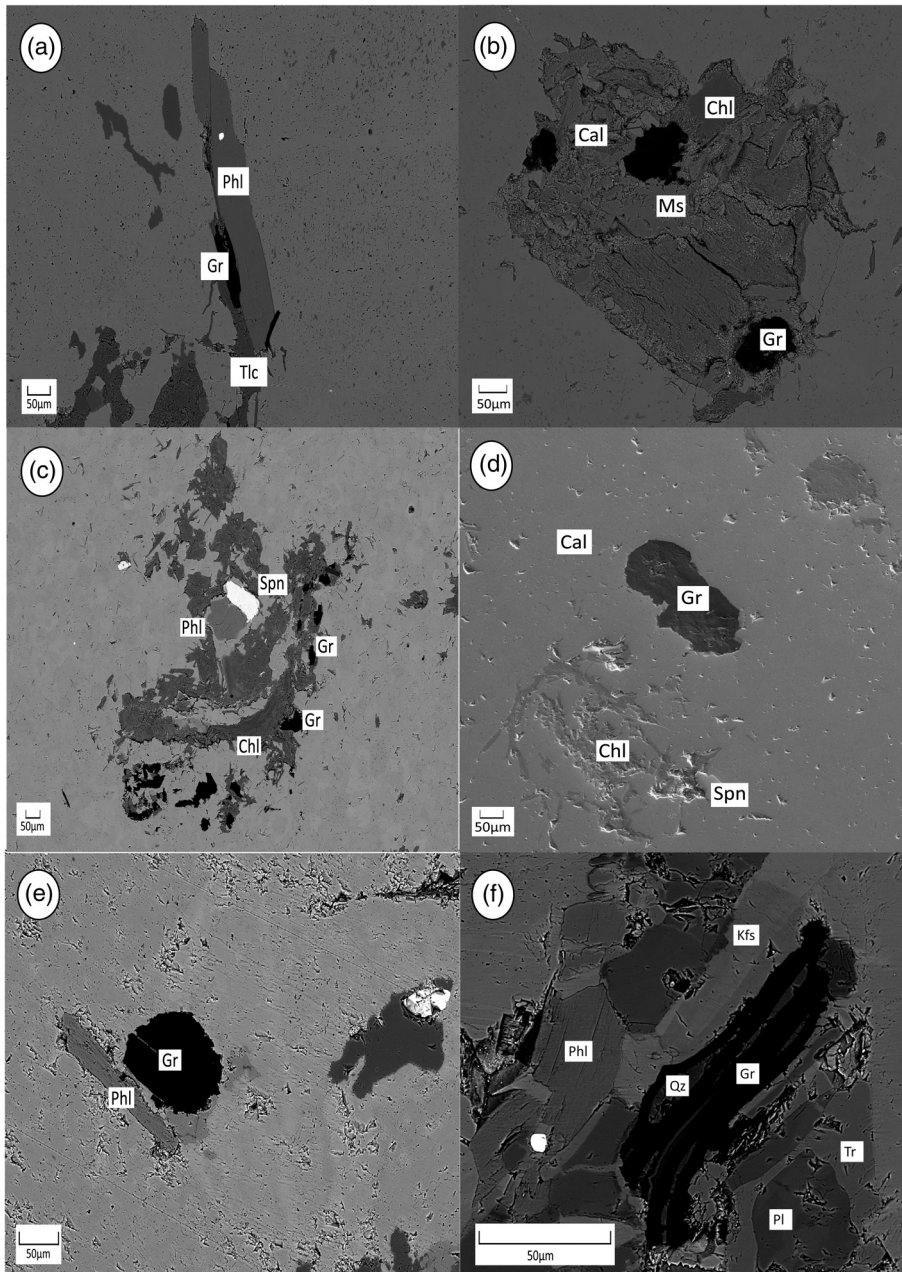


**Fig. 3.** Backscattered electron micrographs of graphite-hosted nodules. (a) Blairhenachrie: graphite in direct contact with phlogopite ± talc in a lath-shaped assemblage. (b) Blairhenachrie: graphite minerals within an aggregate assemblage comprising calcite, altered Mg-chlorite and replacive muscovite. (c) Kirkton: small graphite crystals on the periphery of a Mg-chlorite grain that form a subordinate nodule around central phlogopite and sphene crystals. (d) Kirkton: solitary graphite in a calcite fabric, with a spatial association with Mg-chlorite. (e) Moniak Burn: graphite in direct contact with phlogopite ± talc in a lath-shaped assemblage. (f) Moniak Burn: graphite with thin quartz lenses in an aggregate nodule with phlogopite, and possibly replacive plagioclase, K-feldspar and tremolite. Labels: Cal, calcite; Chl, Mg-chlorite; Gr, graphite; Kfs, K-feldspar; Ms, muscovite; Phl, phlogopite; Pl, plagioclase; Qz, quartz; Spn, sphene; Tlc, talc; Tr, tremolite.

Optical and polarized light microscopy of thin sections was carried out at the University of Aberdeen on a Leica DM750 P microscope, and the photography used a Leica ICC50 E high-resolution imager.

Raman analyses were performed on graphite before and after calcite dissolution by HCl to check the effect of induced disorder on the sample surfaces. Raman analyses were first performed on unpolished cut surfaces and then SEM observations were made. This approach was necessary in order to avoid Raman spectroscopy after polishing. Micro-Raman spectroscopy of graphite samples was carried out at the University of Aberdeen using a Renishaw inVia reflex Raman spectrometer, with a backscattering geometry in the range of  $700\text{--}3200\text{ cm}^{-1}$ , a  $2400\text{ l mm}^{-1}$  spectrometer grating and a CCD detector (Fig. 5). Microscopic observations were carried out with a  $\times 100$  optical power objective with a numerical aperture (NA) of 0.90. The slit opening was  $65\text{ }\mu\text{m}$  with a CCD area of approximately 10 pixels (80% of the total signal height hitting the CCD chip) and the confocal

hole was  $200\text{ }\mu\text{m}$ . A  $514.5\text{ nm}$  diode laser was used for excitation with an output of  $50\text{ mW}$ . Optical filters (10%) were used to adjust the power of the laser to less than  $5\text{ mW}$ . Parameters for the Raman spectra of carbonaceous material were calculated after deconvolution using LabSpec software (Schito *et al.* 2017). Palaeotemperatures (Table 2) were calculated using the conversion of the R2 ratio according to Beysac *et al.* (2002).

Sulfur isotope analysis took place at the Scottish Universities Environmental Research Centre (SUERC), pyrite samples from The Aird were combusted with excess  $\text{Cu}_2\text{O}$  at  $1075^\circ\text{C}$  in order to liberate the  $\text{SO}_2$  gas under vacuum conditions. Liberated  $\text{SO}_2$  gases were analysed on a VG Isotech SIRA II mass spectrometer, with standard corrections applied to raw  $\delta^{66}\text{SO}_2$  values to produce true  $\delta^{34}\text{S}$ . The standards employed were the international standard NBS-123 and IAEA-S-3, and SUERC standard CP-1. For comparison, pyrite sampled from the carbonatite body at Loch Urigill in the Loch Borrallan Complex, during

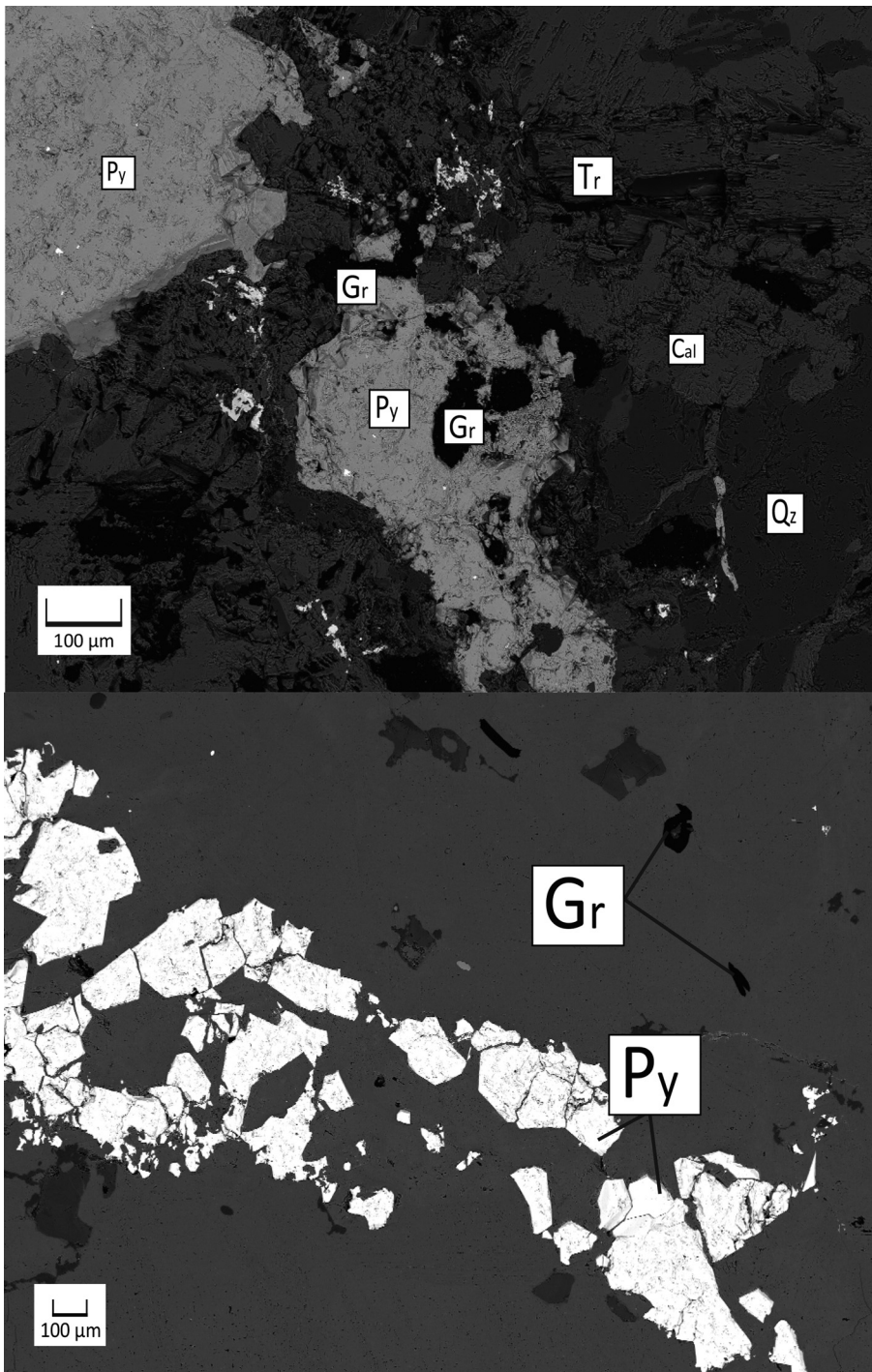


**Fig. 4.** Backscattered electron micrographs of graphite with pyrite in marble, The Aird. (a) Graphite occurs in marble and is entrained in a pyrite vein. The pyrite vein is parallel to a previous calcite vein. (b) Pyrite crystals in a matrix of marble outside the margins of the pyrite vein. Labels: Cal, calcite; Gr, graphite; Py, pyrite; Qz, quartz; Tr, tremolite.

sampling for Heptinstall *et al.* (2023), was also measured (Table 3).

Stable carbon isotope analysis was conducted on graphite samples digested in 10% HCl overnight to remove trace carbonate. Samples were analysed by the standard closed-tube combustion method by reaction in a vacuum with 2 g of wire-form CuO at 800°C overnight. Data are reported in per mil (‰) using the  $\delta$  notation v. Vienna Pee Dee Belemnite (V-PDB). Repeat analysis of the SUERC laboratory standard gave  $\delta^{13}\text{C}$  reproducibility of around  $\pm 0.2\text{‰}$  (1s) (Fig. 6). The graphite samples were collected by dissolving calcite-rich layered marble, which included graphite-phlogopite-enriched layers, entrained graphite in calcite and poorly defined layers of graphite-Mg chlorite  $\pm$  replacive muscovite

(Table 2). However, the technique did permit distinctions between different graphite forms for isotopic analysis. Crystal textural characteristics of graphite minerals recorded in optical, polarized and EDS analysis include mineral assemblage arrangement, and graphite crystal size, shape and presence of twinning or overgrowths.

Fluid-inclusion studies were performed at the University of Aberdeen on doubly polished wafers using a Linkam THMS-600 heating-freezing stage mounted on a Nikon Labophot transmission light microscope. The instrument is equipped with a range of objective lenses, including a  $\times 100$  lens, and was calibrated against synthetic  $\text{H}_2\text{O}$  (374.1 and 0.0°C) and  $\text{CO}_2$  (−56.6°C) standards (Synthetic Fluid Inclusion Reference Set, Bubbles Inc., USA). Approximate

**Table 1** Phlogopite composition by oxide content (wt%: assuming 22 oxygen equivalents) and by atomic units (assuming 11 oxygens per formula in the calculation of phlogopite stoichiometry); the mineral composition is from graphite-associated nodules in The Aird, samples from Moniack Burn, Blairnahanachrie and Kirkton, with specific sample textures and phlogopite crystals in Figure 3

Locality:	Moniack Burn		Blairnahanachrie			Kirkton	
	Layered marble Comparable images: Fig. 3e	Tightly folded marble	Pyrite, bedded marble Fig. 3a			Black, graphitic marble Fig. 3c	
F	2.03		1.39	1.93	1.71	1.10	2.20
MgO	21.68	19.89	24.28	26.05	25.22	21.02	23.8
Al <sub>2</sub> O <sub>3</sub>	15.04	18.06	17.12	16.17	15.47	15.22	16.93
SiO <sub>2</sub>	39.11	41.11	40.57	42.74	41.31	36.28	39.39
K <sub>2</sub> O	8.69	7.33	9.75	10.2	9.76	9.22	9.63
CaO		0.52					
TiO <sub>2</sub>	0.59	0.81	0.67	0.89	0.73	0.48	0.77
FeO	4.18	8.08	0.84	0.88	0.81	0.87	0.81
<b>Sum</b>	<b>91.32</b>	<b>95.80</b>	<b>94.62</b>	<b>98.86</b>	<b>95.01</b>	<b>84.19</b>	<b>93.53</b>
F	1.172		0.717	0.924	0.882	0.72	1.186
Mg	2.418	2.077	2.56	2.645	2.658	2.495	2.565
Al	1.326	1.491	1.427	1.298	1.289	1.428	1.442
Si	2.926	2.88	2.869	2.911	2.921	2.889	2.847
K	0.829	0.655	0.88	0.886	0.88	0.937	0.888
Ca		0.039					
Ti	0.033	0.043	0.036	0.046	0.039	0.029	0.042
Fe	0.261	0.473	0.05	0.05	0.048	0.058	0.049

pressure corrections were made following the approach of Goldstein and Reynolds (1994). Homogenization temperatures were measured by observing the first appearance of a vapour bubble on reheating the homogenized fluid (Table 2).

## Results

### Field observations

Marble exposures in The Aird included a *c.* 4 × 3 m outcrop at Kirkton (NH 606452), a *c.* 3 × 2.5 m outcrop at Rebeg

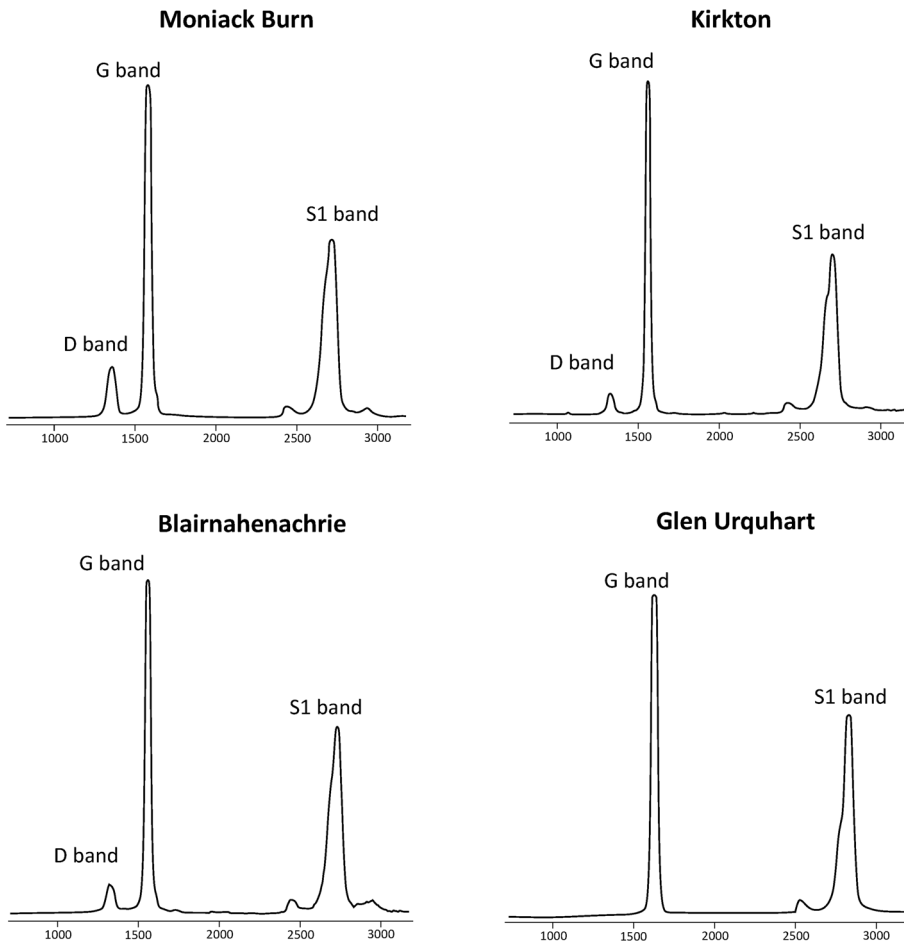


**Fig. 5.** Raman spectra for graphite from Moniack Burn, Kirkton and Blairnahanachrie, all showing a small disorder (D) peak in addition to an order (G) peak and a secondary (S) peak. Spectra for Glen Urquhart are shown for comparison, which lacks a disorder peak.

**Table 2.** Characterization of graphite in The Aird marbles; the graphite associated minerals, carbon isotopic composition and Raman spectroscopic thermometry

Locality	Host	Crystal size (mm)	Graphite associated minerals	Isotopic composition ( $^{13}\text{C}$ ‰)	Raman temperatures ( $^{\circ}\text{C}$ )
Moniack Burn (NH 558425)	Layered marble	0.8	Phlogopite, muscovite, Mg-chlorite, quartz	0.4 to $-1.6$ ( $n = 12$ )	$583 \pm 21$
Blairmahenachrie (NH 597415)	Layered marble	0.5	Phlogopite, Mg-chlorite, pyrite		$589 \pm 15$
Kirkton (NH 606452)	Layered marble	0.8	Phlogopite, Mg-chlorite, pyrite		$590 \pm 20$
Glen Urquhart (NH 484316)	Layered marble	1.0	Kyanite	$-3.4$	$>600$

**Table 3.** Sulfur isotope composition of pyrite; The Aird and adjacent regions

Locality	Grid reference	Sample	Lab No./source	Composition $\delta^{34}\text{S}$ (‰ CDT)
Moniack Burn	NH 558425	Pyrite veinlet in marble	SM 7453	$-15.5$
Moniack Burn	NH 558425	Pyrite veinlet in marble	SM 7463	$-15.7$
Moniack Burn	NH 558425	Pyrite veinlet in marble	SM 7464	$-15.5$
Moniack Burn	NH 558425	Pyrite veinlet in marble	SM 7467	$-16.6$
Moniack Burn	NH 558425	Pyrite veinlet in marble	SM 7468	$-16.6$
Kirkton	NH 606452	Pyrite veinlet in marble	SM 7462	$7.6$
Learnie Quarry, Rosemarkie	NH 736614	Pyrite veinlet in psammite	SM 7447	$7.7$
Learnie Quarry, Rosemarkie	NH 736614	Pyrite veinlet in psammite	SM 7448	$7$
Glen Urquhart	NH 484316	Pyrite in marble coarse calcite (vein?)	SM 7470	$6.1$
Glen Urquhart	NH 484316	Pyrite in marble coarse calcite (vein?)	SM 7471	$6.1$
Blairmahenachrie	NH 597415	Diagenetic pyrite in marble	SM 7465	$0.6$
Blairmahenachrie	NH 597415	Diagenetic pyrite in marble	SM 7466	$0.8$
Loch Urigill	NC 246103	Pyrite in carbonatite	SM 7449	$-5.6$
Loch Urigill	NC 246103	Pyrite in carbonatite	SM 7450	$-5.7$
Strontian		Diagenetic pyrite in ‘Moine’ psammities (Glenfinnan Group rocks)	Lowry <i>et al.</i> (2005)	$+3.4, +4.6$
		Pyrite/pyrrhotite in Strontian Inner Granite	Laouar <i>et al.</i> (1990)	$+5.6, +6.9, +8.5$

Quarry (NH 562422), displaced boulders of marble up to 0.8 m in width at Blairmahenachrie (NH 597415) and Moniack Burn riverbed samples up to  $1.5 \times 0.8 \times 0.6$  m in size (NH 558425). The Kirkton exposure comprises black graphitic marble, interlayered with schist, with veins of hematite and pegmatite. The Rebeg Quarry consists of highly weathered and fissile black marble, with hematite and carbonatite veining. The marble boulders at Blairmahenachrie include a single large block of white, granular marble that showed no discernible layers or veining. Outside of The Aird, samples were collected from centimetre-scale pyrite and carbonatitic veins sampled from psammite in Learnie Quarry (NH 736614). Pyrite and graphite were sampled from marble in the nearby, poorly exposed, Glen Urquhart inlier (NH 484316).

Moniack Burn riverbed debouched boulders are likely to have been transported from the Rebeg and South Clunes quarries further upstream. Moniack Burn comprises

approximately millimetre- to centimetre-scale layers of calcite, dolomite, micaceous minerals, graphitic and pyrite (Fig. 2a). Graphite-rich horizons usually occur in layered calcite marble and calcite–dolomite marble that was later deformed into tight folding. Layered marble samples are cross-cut by both calcite and sulfide veins, which usually followed earlier calcite veins or penetrated along layers in the marble. These calcite and sulfide veins usually occur as *c.* 1–8 cm-long and <1 cm-wide veins in layered marbles. Sulfide veins assimilated graphite from The Aird marbles. Boulder specimens also included basement schist comprising hydrothermal breccia ‘veins’ of comminuted country rock matrix with larger xenoliths of quartzite, schist and macroscopic quartz (also described in Heptinstall *et al.* 2023), all cross-cut by calcite veining (Fig. 2b). Debouched tightly folded marble is cross-cut by undeformed hematite veins (Fig. 2c), which are also present in *in situ* exposures of metasedimentary and marble host rocks in Rebeg Quarry and the Moniack Burn riverbed.

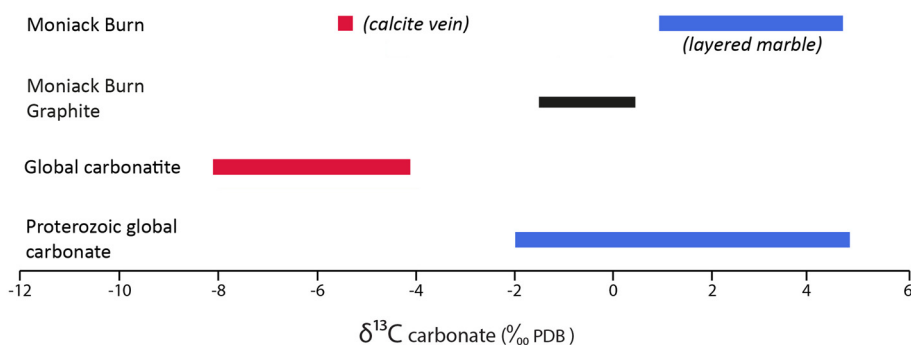


**Fig. 6.** Carbon isotope composition range of graphite hosted in Moniack Burn marble. The carbon isotopic compositions of the Moniack Burn layered marble and cross-cutting (i.e. carbonatite) calcite veins (Heptinstall *et al.* 2023), global carbonatite range (Broom-Fendley *et al.* 2017), and the typical Proterozoic marine carbonate range (Shields and Veizer 2002) shown for comparison. Carbon compositions of limestones and dolostones shown in Shields and Veizer (2002) varied widely between  $-12\text{‰}$  and  $15\text{‰}$  during the time of the Neoproterozoic

Hematite occurs especially in brecciated marble, where it coats the margins of calcite veining, and forms zones of diffuse impregnation in the country rock. Hematite occurs as both deformed veins and impregnations (Fig. 2d), and sub-millimetre width planar veins of hematite (Fig. 2c). However, it is unclear if hematite veining and impregnations occurred during post-Scandian-associated Great Glen Fault deformation, or much younger hematite veining events.

Pegmatites cross-cut outcrops of marble at Kirkton and Rebeg, and boulders in Moniack Burn, ranging from <1 cm to >10 cm in width, are shown to cross-cut marbles at Rosemarkie. Minor brecciation has altered the pegmatite bodies.

## Mineralogy

### Petrographical analysis

Graphite-rich horizons occur in boulders of layered calcite and calcite–dolomite marble in Moniack Burn, and as less distinct horizons and single crystals at Kirkton and Blairnahunachrie. Graphite horizons comprise numerous nodules, commonly with phlogopite (Fig. 2a). Graphitic nodules typically have dimensions of 50  $\mu\text{m}$  up to several hundred micrometres wide (Figs 2a and 3), and can comprise several coalesced graphite crystals. Nodules occur in discrete layers up to several centimetres in length.

Graphite commonly occurs within nodules in association with phlogopite at most localities (Fig. 3a, c, e and f), and also occurs with Mg-chlorite (Fig. 3b, c), pyrite veins (The Aird) (Fig. 4) and kyanite (Glen Urquhart). Smaller quantities of the minerals calcite (Fig. 3b), sphene (Fig. 3c), quartz (Fig. 3f) and replacive muscovite (Fig. 3b) are also present in graphite-hosted nodules. Graphite occurs as lath-shaped (Fig. 3a, c and f) or equidimensional (Fig. 3b–e) crystals. Graphite crystals removed from partly dissolved marble samples exhibited a range of bulbous and platy forms; however, crystallography analysis was not carried out as it is beyond the scope of this work. The graphite does not show overgrowths, and the different graphite forms occur independent of each other, often in layers of the same sample. Collectively, graphite–phlogopite horizons are up to 0.5 cm in width (Fig. 2a).

Graphite crystals commonly occur in lath-shaped assemblages (Fig. 3a); in irregular aggregate assemblages with other silicate and calcite minerals (Fig. 3b); in subordinate assemblages around one or more central silicate crystals (Fig. 3c), where several small graphite crystals may occur at the periphery of phlogopite and Mg-chlorite nodules (Fig. 3c); or as solitary grains in calcite (Fig. 3d). Graphite–phlogopite nodules are the most abundant of the different forms of graphite-bearing nodule identified in marble-hosted rocks of The Aird. Graphite usually occurs with phlogopite but there is much phlogopite with no associated graphite. Graphite also occurs within dark laminae in the marble composed of a meshwork of sub-millimetre quartz and feldspar crystals (Fig. 2a). In places, graphite crystals define the layers and they allow folding to be discerned (Fig. 2c). Graphite-associated phlogopite measured in rocks from The Aird have fluorine (FO) contents of up to 2.2 wt% (Kirkton), 1.93 wt% (Blairnahunachrie) and 2.03 wt% (Moniack Burn) (Table 1); with an approximate

phlogopite stoichiometry of  $\text{K}_{0.655-0.937}\text{Mg}_{2.077-2.658}\text{Al}_{1.289-1.491}\text{Si}_{2.847-2.926}\text{O}_{10}(\text{F}_{0.717-1.186},\text{OH})$ .

Sulfides occur in two settings: as distinct minerals or sub-millimetre scale masses within the layered marble, and as pyrite-rich veins that also host barite and Pb-minerals. Pyrite-rich veins followed calcite veins along layers of the marble country rock (Fig. 2a), and as veins in Learnie Quarry psammite. Graphite inclusions occur within sulfide veins (Fig. 4a) and outside the limits of sulfide veins in layered marble (Fig. 4b). Graphite crystals are typically <100  $\mu\text{m}$  in size, both within (Fig. 4a) and outside of pyrite veins (Fig. 4b).

Calcite veining occurs as mostly linear (Fig. 2a) and, less often, as irregular (Fig. 2b) veins. Calcite veining varies in scale, from *c.* 2–3 cm in width and several centimetres in length to thin (<1 cm) and 3–5 cm-long calcite veins that are shown to comminute the schist matrix (Fig. 2b). Micrometre-scale calcite veins group together into a mass several hundred micrometres wide or splinter off from veins approximately millimetres in width and centimetres in length, that were described in Heptinstall *et al.* (2023) as enriched in Sr, Sc, V, Y, Nb, Ba and REE.

Moniack quartz crystals within breccia zones contained primary two-phase (liquid and vapour) aqueous fluid inclusions up to 10  $\mu\text{m}$  in size (Fig. 2b), from which a mean homogenization temperature of 122.5°C (SD = 9.9°C; *n* = 26) was measured. Petrographical study suggests that quartz mineralization was coeval with brecciation. The homogenization temperature probably equates to at least 150°C after pressure correction. The quartz-bearing fluid inclusions did not contain CO<sub>2</sub>, and so are unlikely to be related to calcite dissolution during metamorphism or calcite veining. They are crosscut by later veins of calcite and smeared out by low-displacement (a few millimetres) small faults (Fig. 2c). Graphite also occurs in some calcite veins filling cross-cutting brittle fractures up to millimetres in width. Tight folding in the marble affecting the calcite–dolomite–graphitic horizons (Fig. 2c) and the early hematite (Fig. 2d) suggests that ductile deformation occurred following graphitization and the intrusion of oxic fluids.

### Optical microscopy

The Moniack Burn (see Fig. A1a in Appendix A), Kirkton (Fig. A1b) and Blairnahunachrie (Fig. A1c) thin sections host tabular to prismatic, phlogopite minerals that occur as light brown crystals in visible light and anisotropic at *c.* 90° extinction angles. Graphite shown in preferential association with phlogopite in a *c.* 1 mm-wide graphitic horizon, occurs as mostly tabular, lath-shaped to equidimensional crystals (Fig. A1a, b). Graphite crystal morphology varies from exhibiting flat edges and apparent basal-pinacoid faces (especially in lath-shaped assemblages) to irregular crystal edges. Monoclinic, <0.5 mm Mg-chlorite crystals occur as light green, prismatic crystals with anomalous (blue–green–yellow) birefringence colours and perfect cleavage parallel to prismatic habit, and comparably higher relief than phlogopite crystals (Fig. A1a, b). Irregular tabular to prismatic colourless calcite crystals vary in size from <0.1 mm up to *c.* 0.5 mm in width and exhibit amorphous (Fig. A1c) to rhombohedral cleavage planes (Fig. A1d), with multiple

twinning and ‘twinkling’ through rotation under polarized light. Calcite in Rosemarkie also exhibits <1 mm clusters of *c.* 0.1 mm calcite and Mg-chlorite crystals surrounded by coarser (*i.e.* *c.* 0.5 mm) calcite crystals (Fig. A1d).

#### Isotope composition

Twelve samples of graphite from marble in The Aird yielded carbon isotope compositions ( $\delta^{13}\text{C}$  ‰) in the range  $-1.6$  to  $0.4\%$  (Table 2; see also Table B1 in Appendix B). These values differ from a carbon isotope composition from graphite in Glen Urquhart ( $-3.4\%$ ) (Table 2) and a carbonatite vein carbon isotope composition in Moniak Burn marble (*c.*  $-5.7\%$ ). The majority of carbon isotopic compositions of Moniak Burn marble are within the range of  $-1.9$  to  $2.6\%$  (Table B1). Eight samples of pyrite (Table 3) from The Aird yielded sulfur isotope  $\delta^{34}\text{S}$  compositions of  $-16.6$  to  $-15.5\%$  CDT ( $n=5$ ) from calcite veins in Moniak Burn, a  $\delta^{34}\text{S}$  composition of  $+7.6\%$  from a single pyrite vein sample at Kirkton and a  $\delta^{34}\text{S}$  composition of  $+0.7\%$  ( $n=2$ ) from pyrite masses in marble at Blairnahenachrie. Pyrite veins in Rosemarkie (Learnie Quarry) psammite and pyrite hosted in coarse calcite at Glen Urquhart had  $\delta^{34}\text{S}$  compositions of  $+7.3\%$  ( $n=2$ ) and  $+6.1\%$  ( $n=2$ ), respectively (Table 3).

#### Graphite Raman analysis

Graphite micro-Raman spectroscopy (Fig. 5) measurements were analysed from several localities in The Aird (Moniak Burn, Kirkton and Blairnahenachrie) and also from Glen Urquhart. Standard parameters for comparing samples and assessing thermal maturation are recorded in Table 2. Raman spectroscopy of samples from The Aird all show a dominant graphite spectrum G-peak but additionally show a small disorder peak. The graphite from Glen Urquhart lacks a disorder peak and is fully graphitized. All graphite spectra additionally show an asymmetrical S1 peak (Fig. 5) in the second-order region. The asymmetry of the S1 band reflects the transition from two- to three-dimensional carbonaceous material that generally occurs at temperatures higher than  $500^\circ\text{C}$  (Wopenka and Pasteris 1993; Satish-Kumar 2005; Ferrari *et al.* 2006). The spectra for The Aird all yielded palaeotemperatures between  $583$  and  $590^\circ\text{C}$ , and higher than  $600^\circ\text{C}$  where pure graphite is present (Glen Urquhart) (Table 2).

Micro-Raman spectroscopic thermometry can be prone to error, including the resolution of the Raman thermometry technique used, which decreases as the limit of  $600^\circ\text{C}$  is approached. We cannot rule out edge effects or surface

effects; however, fully ordered spectra outnumber disordered spectra. No polished surfaces were analysed, as these may be sources of error. Further, in order to confirm fully ordered graphite, analyses were performed on graphite extracted after HCl dissolution and measured on different points of the graphite surface in order to limit edge effects.

## Discussion

### Graphite characterization

#### Carbon isotopic composition of graphite

Despite very different environments of formation, carbonatites and marbles may appear similar and can be confused with each other, particularly in polymetamorphosed terranes (Le Bas *et al.* 2002; Wu 2008), but can be distinguished by isotope and trace element compositions. A carbon isotopic composition  $\delta^{13}\text{C}$  range of  $-1.6$  to  $0.4\%$  (Table 2) in The Aird graphite is consistent with carbon isotopic compositions of calcite ( $\delta^{13}\text{C}$ ,  $-1.9$  to  $2.6\%$ ) in The Aird marble (Fig. 6; see Table B1) and carbonate carbon isotope compositions typical of the Proterozoic (Shields and Veizer 2002), and broadly in line with marble-hosted graphite–phlogopite assemblages elsewhere in the world (Table 4). In contrast, the carbon isotopic composition of marble in Glen Urquhart is close to the  $\delta^{13}\text{C}$  range of mantle-derived carbonatites, with isotopic compositions of  $-3.4\%$ . However, we recognize the uncertainty in carbon isotopic compositions due to limited graphite and calcite sampling at Moniak Burn and other marbles in The Aird (Table B1), especially due to an absence of calcite-enclosed graphite and other carbon isotopic compositions (*i.e.* folded marble  $\delta^{13}\text{C}$ ,  $4.6\%$ ).

The carbon isotopic compositional analysis technique used in this study did not distinguish between calcite-enclosed graphite, graphite nodules with phlogopite and graphite nodules with other micas or Mg-chlorite. The Aird graphite carbon isotopic compositions are outside the  $\delta^{13}\text{C}$  range of  $-10$  to  $-5\%$ , for derivation of graphite from the mantle (Luque *et al.* 2012), or the  $\delta^{13}\text{C}$  range of  $-8$  to  $-4\%$  for carbonatite calcite, as reported by Broom-Fendley *et al.* (2017), or calcite vein (*i.e.* carbonatite) documented in this study with a tight range of carbon isotopic compositions ( $\delta^{13}\text{C}$ ,  $-5.7$  to  $-5.6\%$ ). Carbon isotope compositions of graphite and marble calcite are similar, although a disequilibrium in isotopic compositions between marble calcite ( $\delta^{13}\text{C}$ ,  $1$  to  $4.6\%$ ) and phlogopite nodule-derived graphite crystals ( $\delta^{13}\text{C}$ ,  $-1.6$  to  $0.4\%$ ) is comparable to findings by Satish-Kumar *et al.* (2011). However, unlike Satish-Kumar *et al.* (2011), there is no indication of a second population of

**Table 4.** Isotopic composition of graphite associated with phlogopite; The Aird and marble rocks elsewhere in the world

Locality	Rock type	Associated mica	Carbon isotope (%)	Reference
Udachnaya, Russia	Kimberlite	Phlogopite	$-6.5$ to $-4.0$	Kostrovitsky <i>et al.</i> (2001) and Mikhailenko <i>et al.</i> (2021)
Achankovil, India	Shear zone	Phlogopite	$-9.8$ to $-7.0$	Rajesh <i>et al.</i> (2009)
Western Alps, Italy	Lherzolite	Phlogopite	$-16.1$ to $-10.4$	Ferraris <i>et al.</i> (2004)
Maksyutov Complex, Russia	Eclogite	Phengite–phlogopite	$-42.0$ to $-21.2$	Beane <i>et al.</i> (1995) and Leech and Ernst (1998)
Skallen, East Antarctica	Marble	Phlogopite	$-2.7$ to $-2.5$	Satish-Kumar and Wada (1997)
Naxos, Greece	Marble	Phlogopite	$-7.5$ to $-1.4$	Satish-Kumar <i>et al.</i> (2011)
The Aird, UK	Marble	Phlogopite	$-1.6$ to $0.4$	This study

carbon isotopic compositions, which limits the interpretation of carbon isotopic compositions of graphite in this study.

### The graphite–phlogopite association

The association between graphite and phlogopite at The Aird appears to be due to the preferential precipitation of graphite on/around phlogopite. Both are phases formed during metamorphism, derived from carbon and silicates in the precursor sediments. Preferential precipitation is indicated by:

- (1) Graphite occurs consistently with phlogopite, while there are also many phlogopite-bearing layers with no graphite.
- (2) In some nodular structures, a core rich in phlogopite is surrounded by several smaller crystals of graphite.

The composition of phlogopite can help to distinguish between a mantle or carbonate origin, specifically the F content (Table 1). The fluorine content of some phlogopite grains in Moniack Burn marbles is up to 2.2 wt%, which is typical of compatible behaviour in minerals of a magmatic origin (Dooley and Patino-Douce 1996; Edgar *et al.* 1996; Sun *et al.* 2022). However, most phlogopites in The Aird have compositions of <2 wt% F, which is not diagnostic, or especially indicative, of a magmatic origin (Sun *et al.* 2022). Elsewhere, isochemical fluorine reactions known to occur between fluorine-rich humite group minerals (i.e. norbergite, chondrodite, humite and clinohumite) and phyllosilicates such as phlogopite and amphiboles are known to occur in high-grade marbles, as in the granulite Ambasamudram marble (Satish-Kumar and Niimi 1998). Similar reactions between fluorine-rich humites and phlogopite in granulite-facies marbles could positively skew F contents in marble-derived phlogopite. Norbergite and chondrodite F reactions with amphiboles and phlogopite minerals are also described in the Franklin marble (Kearns *et al.* 1980). However, F-rich humite group minerals may occur in the absence of phlogopite in marbles (Bouregghda *et al.* 2023).

The lath-shaped to equidimensional graphite crystals identified in The Aird marble are most strongly associated with phlogopite (Fig. 3a, c, e and f), in addition to an association with accessory talc (Fig. 3a) or Mg-chlorite (Fig. 3b, c; see also Fig. A1a, b), or, less commonly, calcite (Fig. 3d). Phlogopite occurs as usually well-formed, prismatic crystals with perfect cleavage (Fig. A1a, b). Graphite in The Aird occurs as consistently tabular, lath-shaped to equidimensional crystals within lath-shaped, aggregate or subordinate nodular assemblages, usually with prismatic phlogopite. When compared to ‘well-formed’ tabular, hexagonal and spherical graphite crystals in the Franklin Marble, that comprise basal pinacoid faces typical of flake graphite (Jaszczak 1994, 1997), the graphite crystals in The Aird appear to have a flake-type morphology. The analytical methods in this study cannot constrain in sufficient detail whether graphite crystals in The Aird exhibit basal pinacoid faces that are typical of flake-type graphite in granulite-facies marbles (Jaszczak 1997; Satish-Kumar *et al.* 2011). A more extensive investigation of graphite crystallography in The Aird could add to graphite morphology characterization.

Graphite nodules have similar forms throughout The Aird, commonly as lath-shaped (Fig. 3a), aggregate (Fig. 3b) or subordinate (Fig. 3c) nodular forms, usually in preferential association with phlogopite. Well-formed, accessory minerals, Mg-chlorite (Fig. 3b), quartz (Fig. 3f) and calcite (Fig. 3b), are inliers within aggregate nodules or in graphite crystals, possibly indicative of a carbonate-silicate protolith. Aggregate forms of graphitic nodules rarely are replaced by muscovite (Fig. 3b). It is unclear if the muscovite is retrograde but the poorly formed crystal edges are suggestive of retrograde metamorphism. There is a similar association between graphite and phyllosilicate minerals elsewhere, most notably phlogopite in carbonates, many from high-temperature, granulite-facies ruby-hosted marbles (Yang *et al.* 2019), ruby/corundum-bearing marble (Dzikowski *et al.* 2014) and the sillimanite-bearing Franklin marble (Peck *et al.* 2006).

### Origin of graphite

The preferential association of phlogopite with graphite implies that phlogopite provided the appropriate surface conditions for nucleation and growth of graphite crystals, regardless of the origin of the graphite. Graphite formation by carbonate reduction is discussed by Galvez *et al.* (2013), who described graphitization from a CO<sub>2</sub>-rich fluid by fluid–rock C–O–H hydration reactions between quartz and calcite, generating graphite at temperatures as low as 430°C, and accessory products composed of Ca/Mg-silicates depending on the carbonate protolith composition. Graphite is also documented to precipitate in saturated closed-system C–O–H fluid inclusions (Cesare 1995), which can be correlated depending on the fluid temperature and fluid chemistry, the latter from the fractionation of H<sub>2</sub>O which decreases the fluid density, as the binary H<sub>2</sub>O–CO<sub>2</sub> or H<sub>2</sub>O–CH<sub>4</sub> fluids cross the graphite saturation surface. Carbonates could alternatively have undergone devolatilization through CO<sub>2</sub> and H<sub>2</sub>O volatile exchange between prograde carbonates (i.e. calcite and dolomite) and dehydrated silicate (e.g. micaceous) minerals in associated pelitic rocks, depending on the pressure and temperature gradients, which can drive calcite dissolution, CO<sub>2</sub> fluid release and degassing (Ague 2000; Ague and Nicolescu 2014).

Graphitization associated with carbonate–pelite devolatilization has previously been documented in the mixing of high oxygen fugacity, carbonate-derived CO<sub>2</sub> and low oxygen fugacity metasedimentary-derived CH<sub>4</sub> aqueous fluids, under mid-to high-grade metamorphic facies (e.g. Evans *et al.* 2002; Satish-Kumar 2005), sometimes mineralizing graphite from highly mobile, fracture-bound, carbon-saturated hydrothermal fluids (Rumble *et al.* 1986; Luque *et al.* 2012). Devolatilization mixing of carbonate-derived CO<sub>2</sub> and metasedimentary-derived CH<sub>4</sub> fluids would be likely to deposit graphite that is isotopically lighter than decarbonated carbonate or mantle-derived graphite (Luque *et al.* 2012). Graphite in The Aird is assumed to have formed from decarbonation reactions in an impure carbonate–silicate protolith, forming extensive assemblages of graphite–phlogopite nodules and minor graphite associations with accessory minerals, Mg-chlorite and talc. Devolatilization-associated graphitization in The Aird is unlikely, due to possibly limited volatile exchange with carbon-poor Loch

Ness Supergroup pelitic rocks; a lack of fracture-bound, isotopically light graphite; and graphite-associated accessory mineralogies that are consistent with decarbonation reactions between a calcite and quartz-enriched protolith (e.g. Galvez *et al.* 2013). However, the fluid–rock characteristics that influence the CO<sub>2</sub>–phlogopite preferential association remain underexplored in decarbonated marbles, especially in the absence of reduced organic carbon or mantle-derived fluids (e.g. Satish-Kumar *et al.* 2011; Galvez *et al.* 2013).

The original *c.* 870 Ma limestone would have undergone two or three orogenic episodes prior to the Great Glen Fault-associated deformation (i.e. post-Scandian) (Strachan *et al.* 2010; Mako *et al.* 2021; Krabbendam *et al.* 2022). It is also plausible that isotopic compositions recorded in graphite and sulfide minerals may have been reset by post-Grampian I/II dissolution and reprecipitation. Pressure and temperature constraints during the Knoydartian Orogeny for Lower psammite, Morar pelite and Upper psammite rocks in the Morar Group, in the Wester Ross Supergroup (Krabbendam *et al.* 2022), are suggested by Cutts *et al.* (2009) to have reached *c.* 7.5 kbar and 650°C, respectively. This was prior to or during garnet growth, associated with an early extensional regime, followed by crustal thickening. Monazite–xenotime thermometry of the Loch Eil Group and Glenfinnan Group rocks in the Naver Nappe are recognized by Mako *et al.* (2019) to have experienced decompression heating from 8–9 kbar and 600°C to 6–7 kbar and 700°C, with peak metamorphism occurring at *c.* 425 Ma. Different temperature constraints occur in monazite and xenotime elsewhere in the Sgurr Beag Nappe (Mako *et al.* 2021), which could have had the effect of forming two or more distinct trace element compositions and geochronologies.

The presence of well-formed Mg-chlorite and talc as accessory associated minerals, rather than as later replacive assemblages, is suggestive of decarbonation reactions between protolith carbonate and silicate minerals. The origin of graphite is also constrained by the low graphite contents in surrounding Glenfinnan Group metasedimentary rocks. However, the pelitic rocks cannot be ruled out as an external source of CO<sub>2</sub> fluids. Graphitization in The Aird is likely to have formed from a decarbonated CO<sub>2</sub>-rich fluid, given the tight carbon isotopic range of graphite minerals and the apparent absence of carbon isotopic zoning. Graphitization possibly occurred during a single phase, although this may not correlate to peak metamorphism, given a noticeable disequilibrium in graphitic carbon isotopic compositions compared to marble calcite isotopic compositions.

#### Raman and fluid-inclusion thermometry

The Raman spectra indicate almost complete ordering of the graphite at The Aird. The slight disorder, although not observed in the graphite from Glen Urquhart, is not sufficiently marked to be certain that they have experienced different degrees of metamorphism. Peak metamorphic temperatures in The Aird of *c.* 580–600°C, inferred from Raman spectroscopy, is an appropriate temperature range for amphibolite-facies metamorphism (Luque *et al.* 2012). However, there is a decrease in temperature resolution as the limit of 600°C is approached. Raman spectroscopy geothermometry measurements taken from The Aird marble

and Loch Ness Supergroup pelitic rocks suggests the rocks underwent mid–upper amphibolite-facies metamorphism during the Grampian Orogeny, with predicted similar peak temperatures of *c.* 600°C (Strachan *et al.* 2010; Chew and Strachan 2014). The main assumption of Raman geothermometry in this study is that the ordering of graphite is a function of metamorphic temperatures, and that disorder in graphite corresponds to temperatures generally lower than 650°C. Our data indicate that after graphite precipitation in The Aird, the highest metamorphic temperatures were recorded in the Glen Urquart graphite. No interpretation is possible of temperatures above the limit of full graphitization, nor can we precisely assess the metamorphic degree. However, we can give some information about different ranks reached after graphite precipitation.

Homogenization temperatures established through two-phase (liquid and vapour) aqueous fluid inclusions in breccia-hosted quartz crystals suggest mean homogenization temperatures of 122.5°C (*c.* 150°C after pressure correction), far below the temperature of graphite indicated by Raman spectroscopy. No positive identification of carbon-derived fluids is indicated by aqueous fluid inclusions hosted in breccia-hosted quartz crystals, which together with significantly cooler thermometry, below those measured by Galvez *et al.* (2013), suggests that fluid inclusions are likely to be unrelated to regional metamorphism-derived graphitization in The Aird. Fluid-inclusion thermometry suggests that brecciation is likely to have occurred during post-Scandian shearing.

#### Accompanying sulfides

The sulfur isotope data indicate several populations of pyrite. The vein-hosted pyrite consists of a light population from Moniak Burn ( $\delta^{34}\text{S}$ , –16.6 to –15.5‰) and a moderately heavy ( $\delta^{34}\text{S}$ , 6–8‰) population evident at Kirkton, and also Glen Urquhart and Rosemarkie (Table 3). The diagenetic pyrite in Blaimahenachrie carbonate has a near-zero composition compared to the vein pyrite. The moderately heavy pyrite sampled from Kirkton, Glen Urquhart and Rosemarkie is comparable to pyrite mineralized in the Caledonian Strontian Granite 100 km to the SW, also along the Great Glen Fault (Laouar *et al.* 1990). The heavier measurements here are also similar to values from pyrite in the ‘Moine’ (Lowry *et al.* 2005), which may suggest that pyrite veining along the Great Glen Fault was mobilized from elsewhere in the Loch Ness Supergroup.

The vein pyrite from Moniak Burn has a composition that is light enough to suggest biogenic processing of sulfur, which may have remobilized into the veins from a layered source. A succession in the close vicinity of The Aird with evidence of biogenic pyrite is the *c.* 400 Ma Lower Old Red Sandstone at Strathpeffer (Parnell 1985). Neither vein set at Moniak Burn and Kirkton matches the composition of the mantle-derived pyrite at Loch Urigill in the Loch Borralan Alkaline Complex, which is within the  $\delta^{34}\text{S}$  –6 to +3‰ CDT range of most carbonatite-hosted pyrite (Farrell *et al.* 2010; Gomide *et al.* 2013). The sulfide vein fluids at The Aird are therefore unlikely to be mantle-derived, and are more likely to be associated with shallow (crustal) fluid–rock interactions with Glenfinnan metasedimentary rocks. Graphite

entrained in pyrite veins is also likely to have been remobilized from the marble by sulfide fluids, given the similar graphite grain morphologies in both the pyrite vein and the marble host rock.

### Paragenesis

Graphitization is assumed to have occurred in a single episode of metamorphism during the Grampian Orogeny, and is likely to have occurred at a similar time to ductile deformation, at peak metamorphism temperatures of *c.* 580–600°C that are typical of mid–upper amphibolite-facies metamorphism (Luque *et al.* 2012). Graphitization associated with the Scandian Orogeny appears to have insufficient evidence of ductile shearing that was sufficient for greenschist–amphibolite-facies metamorphism, given the petrographical evidence of brittle deformation features and aqueous fluids identified in quartz grains within hydraulic breccia that do not contain any CO<sub>2</sub>. So it is not possible to confirm directly that graphitization occurred from a CO<sub>2</sub>-rich fluid from an external source. The graphite carbon isotopic composition strongly supports a sedimentary carbonate source, as discussed above, as there is insufficient mineralogical and carbon isotopic compositional evidence of graphitization associated with mantle-derived carbonatite magmatism.

The pyrite in the matrix of the marble consists of coalesced crystals, interpreted as having formed during burial diagenesis, and which are unrelated to later sulfide veining. The graphite and phlogopite were products of subsequent metamorphism. Graphitization-associated metamorphism of the Loch Ness Supergroup, especially in the Glenfinnan Group, as in The Aird, may have occurred in the Grampian I event between *c.* 470 and 460 Ma (Strachan *et al.* 2010; Mako *et al.* 2021). However, overprinting of Knoydartian fabric (Cutts *et al.* 2010) or evidence of Grampian II orogenesis (Bird *et al.* 2013; Milne *et al.* 2023) is limited. Future Re–Os geochronology investigations of pyrite in The Aird may further constrain pre-Caledonian and Grampian I/II orogenic reworking of The Aird marble.

Fluid inclusions within breccia-hosted quartz crystals and folded hematite veins in The Aird marbles imply that the rocks in The Aird underwent post-Scandian hydraulic brecciation and hematite deposition *transitional to* the alkaline and carbonatitic mineralization reported in Heptinstall *et al.* (2023). Fluid inclusions in authigenic quartz within breccia suggest a temperature for brittle deformation of about 150°C (Table 5). Brecciation and hematite veining in The Aird may correlate with the partitioning of transpressive strain and sinistral displacements described along the Great Glen Fault that post-dates

Scandian ductile thrusting (Strachan *et al.* 2010, 2020a, b). The timing of Scandian to post-Scandian sinistral motion on the Great Glen Fault is constrained to have begun as early as *c.* 428 Ma, marked by emplacement of the Clunes tonalite (Stewart *et al.* 2001), and continued until at least *c.* 399 Ma, marked by syndeformational emplacement of granite veins at Rosemarkie (Mendum and Noble 2010). Recent U–Pb zircon dating of the Abriachan Granite by MacRae *et al.* (2023) argues for emplacement at  $420.1 \pm 3.4$  Ma. Consequently, shearing, calcite veining, pyrite veining and especially fenitization recorded in the Abriachan Granite (Garson *et al.* 1984) and The Aird (Heptinstall *et al.* 2023) may have occurred between *c.* 420 and *c.* 399 Ma. While there is some suggestion of earlier hematite veining, based on petrographical relationships, the majority is post-Devonian.

Hematite veining is found through the region west of the Great Glen Fault at Loch Ness, and in Badenoch Group metasediments and Devonian sediments, although these examples are unfolded (Elmore *et al.* 2006). Palaeomagnetic studies of the Devonian sediments immediately west of Loch Ness in the Mealfaurvonie Outlier indicate that the hematite is of Carboniferous–Permian age (Elmore *et al.* 2006). Widespread reddening by hematite from above at this time reflects uplift and basin inversion related to the Hercynian Orogeny (Dichiarante *et al.* 2020). Recent radiometric dating (e.g. Mendum and Noble 2010; MacRae *et al.* 2023), carbonatitic-related mineralization (Garson *et al.* 1984; Heptinstall *et al.* 2023) and petrographical findings of post-orogenic modification by brittle deformation in this study do not all correlate to pre-existing Great Glen Fault kinematics (e.g. Stewart *et al.* 2001; Strachan *et al.* 2010, 2020a). We propose that the findings in this study may be further constrained through radiometric dating and by assigning brecciation, fenitization, veining of crustal fluids and shearing textures to sinistral or dextral transpressional or transtensional deformation regimes of the Great Glen Shear Zone, and stratigraphic correlation to sinistral or dextral movement of the Great Glen Fault.

Given these constraints, the paragenesis can be summarized from the rock descriptions (Table 5) as:

- (1) diagenesis, including pyritization;
- (2) metamorphism in Grampian I, including precipitation of graphite and phlogopite; however the phlogopite surface conditions attributed to preferential precipitation of graphite from CO<sub>2</sub> fluids remain underexplored in decarbonated marbles;
- (3) late Scandian hydraulic brecciation of rocks with deposition of hematite (after 428 Ma), *transitional to*;

**Table 5.** Paragenetic sequence in graphite-bearing marbles in The Aird

Stage	Deformation history	Mineral phases	Temperature (°C)	Reference	Timing (Ma)
1 Sedimentation, diagenesis	Burial	Calcite, detrital grains, pyrite	<50	Near surface	900–870
2 Metamorphism	Ductile deformation	Graphite, micas, amphiboles	<i>c.</i> 600	This study	475–460
3 Brecciation, transitional to and approximately coeval with fenitization	Brittle brecciation	Hematite, vein calcite, pyrite, graphite, magnesioriebeckite	<i>c.</i> 150+	This study	<i>c.</i> 420–399
4 Uplift	Late brittle	Hematite	<100	Near surface	From <i>c.</i> 399

- (4) fenitization (e.g. Heptinstall *et al.* 2023) accompanied by calcite veining, pyrite veining and graphite remobilization from *c.* 420 to 399 Ma;
- (5) local shearing and brittle faulting associated with the Great Glen Fault in the Loch Ness region, from *c.* 399 Ma; and
- (6) further hematite mineralization, possibly *coeval* with Carboniferous–Permian hematite mineralization in the Mealfaurvonic Outlier.

#### Graphite host rocks

Previous observations have linked the decarbonation of protolith carbonate during amphibolite-facies regional metamorphism to the Grampian event (Rock *et al.* 1986b; Cutts *et al.* 2010; Strachan *et al.* 2010; Goodenough *et al.* 2011). Descriptions of Loch Ness Supergroup graphitic marbles in The Aird, and marbles elsewhere in the Northern Highlands Terrane including the Lewisian-age Scardroy Inlier and distinct Neoproterozoic Glen Urquhart marble, indicate that graphite is more widespread in northern Scotland than previously identified. Graphite crystals and their nodular assemblages occur in several forms, including graphite–phlogopite horizons up to 0.5 cm in width. In these horizons, graphite nodules are usually associated with phlogopite, talc or Mg-chlorite.

The rocks west of Loch Ness exhibit tight folding, brecciation and shearing, orientated particularly parallel to the fault. The Devonian sediments are also deformed by the tight folding (Mykura and Owens 1983). However, the tight folding in The Aird marble is much more ductile than in the Devonian, suggesting ductile deformation occurred prior to the Devonian, when there was further brecciation and shearing (Stewart *et al.* 1999; Mendum and Noble 2010). The deformation along the Great Glen Fault represents repeated episodes of strike-slip movement and brittle faulting, and there is no requirement to conflate different folding events (Stewart *et al.* 1999; Strachan *et al.* 2010).

Ductile deformation occurred at a similar time to peak metamorphism and graphitization between 475 and 460 Ma (Cutts *et al.* 2010; Mendum and Noble 2010). This is supported by dating of a pegmatite in The Aird at  $463 \pm 4$  Ma by Cutts *et al.* (2010) and a monazite age of  $473 \pm 2$  Ma in Glen Urquhart (Mako *et al.* 2021). However, we cannot rule out that ductile deformation documented in The Aird is associated with later (Scandian) movement of the Moine Thrust, at *c.* 430 Ma (Goodenough *et al.* 2011). The period of brecciation, fenitization, calcite veining and pyritization with graphite remobilization also occurred during the Caledonian Orogeny but before Devonian sedimentation (Garson *et al.* 1984; Heptinstall *et al.* 2023).

#### Conclusions

The graphite–phlogopite association is recorded in Proterozoic marble at The Aird, in the Northern Highland Terrane, Scotland. The occurrence supports previous suggestions that graphite and phlogopite show a preferred relationship. We have shown:

- (1) The carbon at The Aird is derived from decarbonation of protolith carbonate, with graphitization derived

from a CO<sub>2</sub>-rich fluid that had similar carbon isotopic compositions to the host marble, and the isotopic composition range of sedimentary carbonates in the Proterozoic.

- (2) Graphite and phlogopite formed during amphibolite metamorphism of Proterozoic limestone at temperatures of nearly 600°C, at or prior to *c.* 470 Ma (*c.* Grampian I). Well-formed minerals Mg-chlorite and talc are also likely to have been mineralized *coeval* to amphibolite-facies metamorphism and graphitization, given the few retrograde textures (i.e. replacive muscovite). Graphites in The Aird are unlikely to be synchronous with breccia-hosted, quartz-derived fluid inclusions of indeterminate composition that suggest fluid temperatures of *c.* 150°C.
- (3) Three distinct sulfide populations are present in The Aird marbles. Two sulfur isotopic compositions are attributed to veins that post-date graphitization: a light population suggestive of a biogenic source and which is likely to have been derived from crustal fluid–rock interactions, and a heavy population suggestive of a mantle origin. Near-zero sulfur isotopes are likely to have been derived from a diagenetic source in the marble protolith.
- (4) The marbles of The Aird underwent extensive post-Scandian hydraulic brecciation and hematite deposition after *c.* 428 Ma: that is, *transitional* to calcite veining, pyrite veining and fenitization by mantle-derived alkaline and carbonatitic fluids, between *c.* 420 and *c.* 399 Ma. The graphite in the marble predates cross-cutting veins of calcite attributed to carbonatite-related fluids following the Scandian Orogen. Any graphite in calcite or sulfide veins is probably incorporated from the country rocks.
- (5) Subsequent uplift, shearing (i.e. folded hematite veins), late brittle faulting and undeformed brecciation is likely to be associated with the Great Glen Fault, from *c.* 399 Ma, as described in Glenfinnan Group rocks along the Great Glen Shear Zone. Further hematite deposition by <100°C oxidizing fluids occurred later, possibly during the late Carboniferous–early Permian.

*Scientific editing by Iain Neill*

**Acknowledgements** We are grateful to J. Still, J. Johnston and J. Bowie for skilled technical support. We are grateful for previous reviews by Eimear Deady and an anonymous reviewer during an earlier proof, and to the reviewers of this paper for their constructive suggestions.

**Author contributions** EAH: conceptualization (equal), data curation (equal), formal analysis (lead), investigation (lead), methodology (equal), project administration (equal), software (equal), validation (lead), visualization (equal), writing – original draft (lead), writing – review & editing (equal); JP: conceptualization (equal), funding acquisition (lead), methodology (equal), project administration (equal), resources (equal), supervision (lead), visualization (equal), writing – original draft (supporting), writing – review & editing (equal); AS: data curation (equal), investigation (supporting), methodology (equal), software (equal); AJB: data curation (equal), formal analysis (supporting); JGTA: data curation (equal), formal analysis (supporting), methodology (equal); DM: formal analysis (supporting).

**Funding** This work was funded by the Natural Environmental Research Council (grant No. NE/M010953/1 awarded, in partial support, to J.P.). The isotope facility at SUERC is supported by NERC.

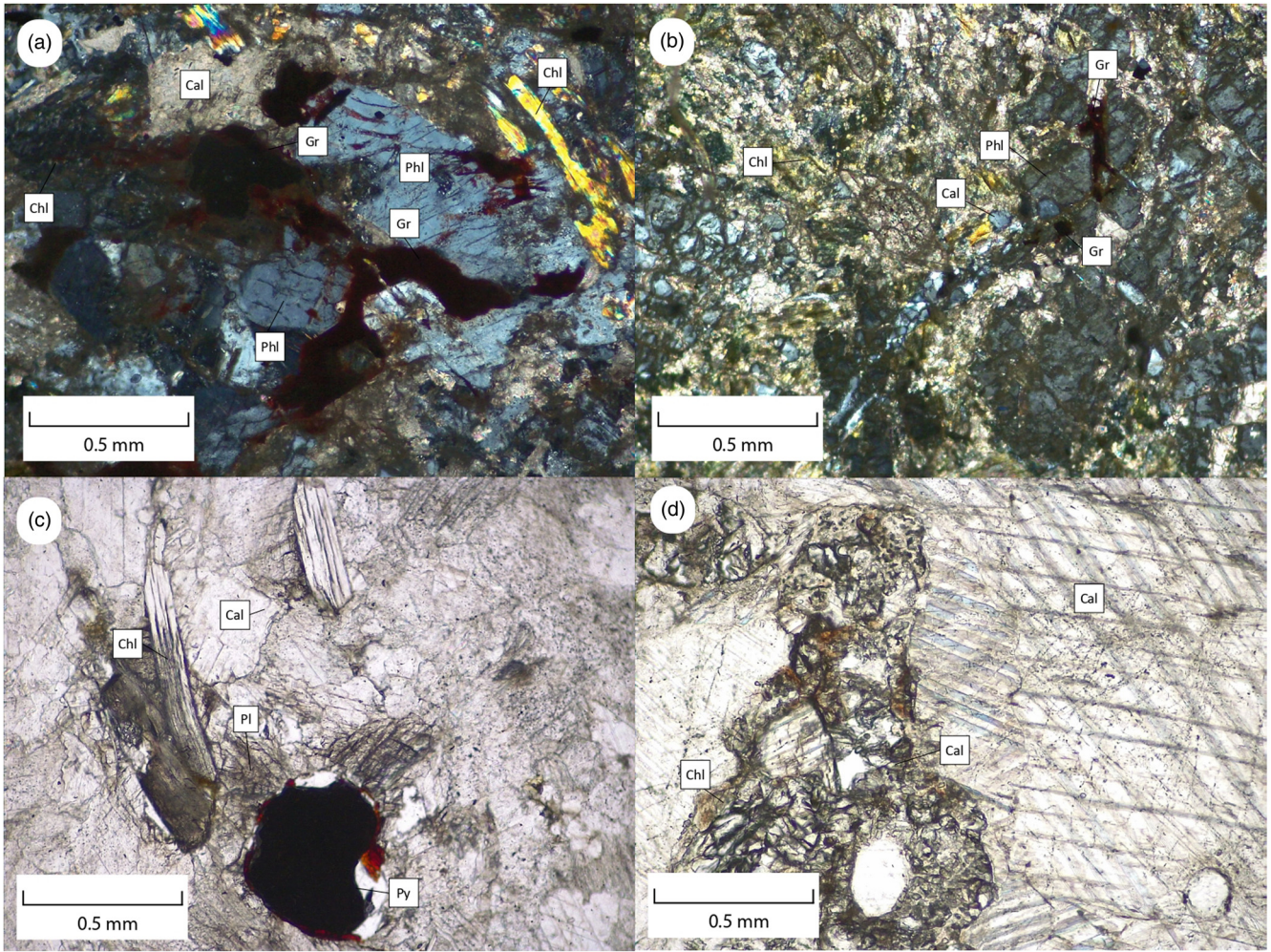


**Fig. A1.** Marble thin-section photographs viewed under a Leica DM750 P microscope. (a) Graphite–phlogopite nodules with accessory Mg-chlorite in a Moniack Burn thin section, viewed under polarized light. (b) Graphite–phlogopite nodules within a calcite–Mg-chlorite fabric in a Kirkton thin section, viewed under polarized light. (c) Cubic pyrite with prismatic plagioclase crystals that exhibit multiple twinning and accessory Mg-chlorite in a Blairnahanachrie thin section, viewed under visible light. (d) Calcite and Mg-chlorite nodules hosted within a coarse calcite fabric in a Rosemarkie thin section, viewed under visible light.

**Table B1.** Carbon isotopic compositions ( $\delta^{13}\text{C}$  ‰) of graphite in marble, calcite fabric in marble and calcite in carbonatitic veins from Moniack Burn graphitic horizons, with relevant sample codes and sampling locations

Sample code	Rock	Mineral	Location	Carbon isotopic composition ( $\delta^{13}\text{C}$ ‰)
PPGraphite01	Marble	Graphite	Moniack Burn	-1.4
PPGraphite02	Marble	Graphite	Moniack Burn	-1.4
PPGraphite03	Marble	Graphite	Moniack Burn	-1.3
PPGraphite04	Marble	Graphite	Moniack Burn	-1.5
PPGraphite05	Marble	Graphite	Moniack Burn	-1.6
PPGraphite06	Marble	Graphite	Moniack Burn	-0.1
PPGraphite07	Marble	Graphite	Moniack Burn	0
PPGraphite08	Marble	Graphite	Moniack Burn	-0.2
PPGraphite09	Marble	Graphite	Moniack Burn	-0.9
PPGraphite10	Marble	Graphite	Moniack Burn	-1.2
PPGraphite11	Marble	Graphite	Moniack Burn	0.3
PPGraphite12	Marble	Graphite	Moniack Burn	0.4
PPMAR35	Marble	Calcite	Blairnahanachrie	-1.9
PPMAR89	Marble	Calcite	Moniack Burn	2.6
PPMAR90	Marble	Calcite	Moniack Burn	1
PPMAR36	Marble	Calcite	Moniack Burn (folded)	4.6
PPMAR85	Carbonatite vein	Calcite	Moniack Burn	-5.7
PPMAR86	Carbonatite vein	Calcite	Moniack Burn	-5.6
PPMAR87	Carbonatite vein	Calcite	Moniack Burn	-5.6
PPMAR88	Carbonatite vein	Calcite	Moniack Burn	-5.7

**Competing interests** The authors declare that they have no known competing financial interests or personal relationships that could have appeared to influence the work reported in this paper.

**Data availability** All data generated or analysed during this study are included in this published article (and, if present, its supplementary information files).

## Appendix A

Thin-section photographs of the marble are shown in Figure A1.

## Appendix B

Graphite isotopic compositions for samples taken from Moniack Burn are shown in Table B1.

## References

- Ague, J.J. 2000. Release of CO<sub>2</sub> from carbonate rocks during regional metamorphism of lithologically heterogeneous crust. *Geology*, **28**, 1123–1126, [https://doi.org/10.1130/0091-7613\(2000\)28<1123:ROCFRCR>2.0.CO;2](https://doi.org/10.1130/0091-7613(2000)28<1123:ROCFRCR>2.0.CO;2)
- Ague, J.J. and Nicolescu, S. 2014. Carbon dioxide released from subduction zones by fluid-mediated reactions. *Nature Geoscience*, **7**, 355–360, <https://doi.org/10.1038/ngeo2143>
- Ashchepkov, I.V., Logvinova, A.M. *et al.* 2015. The Sytykanskaya kimberlite pipe: evidence from deep-seated xenoliths and xenocrysts for the evolution of the mantle beneath Alakit, Yakutia, Russia. *Geoscience Frontiers*, **6**, 687–714, <https://doi.org/10.1016/j.gsf.2014.08.005>
- Beane, R.J., Liou, J.G., Coleman, R.G. and Leech, M.L. 1995. Petrology and retrograde P–T path for eclogites of the Maksyutov Complex, Southern Ural Mountains, Russia. *Island Arc*, **4**, 254–266, <https://doi.org/10.1111/j.1440-1738.1995.tb00148.x>
- Belley, P.M., Dzikowski, T.J. *et al.* 2017. Origin of scapolite-hosted sapphire (corundum) near Kimmirut, Baffin Island, Nunavut, Canada. *The Canadian Mineralogist*, **55**, 669–699, <https://doi.org/10.3749/canmin.1700018>
- Beyssac, O., Goffé, B., Chopin, C. and Rouzaud, J.N. 2002. Raman spectra of carbonaceous material in metasediments: a new geothermometer. *Journal of Metamorphic Geology*, **20**, 859–871, <https://doi.org/10.1046/j.1525-1314.2002.00408.x>
- Bird, A.F., Thirlwall, M.F., Strachan, R.A. and Manning, C.J. 2013. Lu–Hf and Sm–Nd dating of metamorphic garnet: evidence for multiple accretion events during the Caledonian orogeny in Scotland. *Journal of the Geological Society, London*, **170**, 301–317, <https://doi.org/10.1144/jgs2012-083>
- Bird, A., Cutts, K., Strachan, R., Thirlwall, M.F. and Hand, M. 2018. First evidence of Renlandian (c. 950–940 Ma) orogeny in mainland Scotland: implications for the status of the Moine Supergroup and circum-North Atlantic correlations. *Precambrian Research*, **305**, 283–294, <https://doi.org/10.1016/j.precamres.2017.12.019>
- Bird, A., Thirlwall, M., Strachan, R.A., Millar, I.L., Dempsey, E.D. and Hardman, K. 2023. Eclogites and basement terrane tectonics in the northern arm of the Grenville orogen, NW Scotland. *Geoscience Frontiers*, **14**, 101668, <https://doi.org/10.1016/j.gsf.2023.101668>
- Bouregghda, N., Ouzegane, K., Ait-Djafer, S., Bendaoud, A., Zoheir, B.A. and Kienast, J.R. 2023. Ba-rich phlogopite, dissakisite-(Ce), and fluorine-rich clinohumite in granulite-facies marbles from the In Ouzal terrane, Western Hoggar, Algeria. *Mineralogy and Petrology*, **117**, 99–111, <https://doi.org/10.1007/s00710-022-00802-1>
- Brook, M. and Rock, N.M.S. 1983. Caledonian ages for pegmatites in the Glen Urquhart serpentinite-metamorphic complex, Inverness-shire. *Scottish Journal of Geology*, **19**, 327–332, <https://doi.org/10.1144/sjg19030327>
- Broom-Fendley, S., Wall, F., Spiro, B. and Ullmann, C.V. 2017. Deducing the source and composition of rare earth mineralising fluids in carbonatites: insights from isotopic (C, O, <sup>87</sup>Sr/<sup>86</sup>Sr) data from Kangankunde, Malawi. *Contributions to Mineralogy and Petrology*, **172**, 96, <https://doi.org/10.1007/s00410-017-1412-7>
- Cawood, P.A., Nemchin, A.A., Strachan, R.A., Kinny, P.D. and Loewy, S. 2004. Laurentian provenance and an intracratonic tectonic setting for the Moine Supergroup, Scotland, constrained by detrital zircons from the Loch Eil and Glen Urquhart successions. *Journal of the Geological Society, London*, **161**, 861–874, <https://doi.org/10.1144/16-764903-117>
- Cawood, P.A., Strachan, R.A. *et al.* 2015. Neoproterozoic to early Palaeozoic extensional and compressional history of East Laurentian margin sequences: The Moine Supergroup, Scottish Caledonides. *Geological Society of America Bulletin*, **127**, 349–371, <https://doi.org/10.1130/B31068.1>
- Cesare, B. 1995. Graphite precipitation in C–O–H fluid inclusions: closed system compositional and density changes, and thermobarometric implications. *Contributions to Mineralogy and Petrology*, **122**, 25–33, <http://www.eurispet.eu/Bernardo/cesare1995>, <https://doi.org/10.1007/s004100050110>
- Chew, D.M. and Strachan, R.A. 2014. The Laurentian Caledonides of Scotland and Ireland. *Geological Society, London Special Publications*, **390**, 45–91, <https://doi.org/10.1144/SP390.16>
- Cutts, K.A., Hand, M., Kelsey, D.E. and Strachan, R.A. 2009. Orogenic versus extensional settings for regional metamorphism: Knoydartian events in the Moine Supergroup revisited. *Journal of the Geological Society, London*, **166**, 201–204, <https://doi.org/10.1144/0016-76492008-015>
- Cutts, K.A., Kinny, P.D. *et al.* 2010. Three metamorphic events recorded in a single garnet: integrated phase modelling, in-situ LA-ICPMS and SIMS geochronology from the Moine Supergroup, NW Scotland. *Journal of Metamorphic Geology*, **28**, 249–267, <https://doi.org/10.1111/j.1525-1314.2009.00863.x>
- Deans, T., Garson, M.S. and Coats, J.S. 1971. Fenite-type soda metamorphism in the Great Glen, Scotland. *Nature*, **234**, 145–147, <https://doi.org/10.1038/physci234145a0>
- Dewey, J.F. and Strachan, R.A. 2003. Changing Silurian–Devonian relative plate motion in the Caledonides: sinistral transpression to sinistral transtension. *Journal of the Geological Society, London*, **160**, 219–229, <https://doi.org/10.1144/0016-764902-085>
- Dichiarante, A.M., Holdsworth, R.E. *et al.* 2016. New structural and Re–Os geochronological evidence constraining the age of faulting and associated mineralization in the Devonian Orcadian Basin, Scotland. *Journal of the Geological Society, London*, **173**, 457–473, <https://doi.org/10.1144/jgs2015-118>
- Dichiarante, A.M., Holdsworth, R.E., Dempsey, E.D., McCaffrey, K.J.W. and Utley, T.A.G. 2020. Outcrop-scale manifestations of reactivation during multiple superimposed rifting and basin inversion events: the Devonian Orcadian Basin, northern Scotland. *Journal of the Geological Society*, **178**, <https://doi.org/10.1144/jgs2020-089>
- Dooley, D.F. and Patino-Douce, A.E. 1996. Fluid-absent melting of F-rich phlogopite + rutile + quartz. *American Mineralogist*, **81**, 202–212, <https://doi.org/10.2138/am-1996-1-225>
- Doroshkevitch, A.G., Wall, F. and Ripp, G.S. 2007. Magmatic graphite in dolomite carbonatite at Pogranichnoe, North Transbaikalia, Russia. *Contributions to Mineralogy and Petrology*, **153**, 339–353, <https://doi.org/10.1007/s00410-006-0150-z>
- Dzikowski, T.J., Cempirek, J., Groat, L.A., Dipple, G.M. and Giuliani, G. 2014. Origin of gem corundum in calcite marble: the Revelstoke occurrence in the Canadian Cordillera of British Columbia. *Lithos*, **198–199**, 281–297, <https://doi.org/10.1016/j.lithos.2014.03.030>
- Edgar, A.D., Pizzolato, L.A. and Sheen, J. 1996. Fluorine in igneous rocks and minerals with emphasis on ultrapotassic mafic and ultramafic magmas and their mantle source regions. *Mineralogical Magazine*, **60**, 243–257, <https://doi.org/10.1180/minmag.1996.060.399.01>
- Elliott, H.A.L., Wall, F. *et al.* 2018. Fenites associated with carbonatite complexes: a review. *Ore Geology Reviews*, **93**, 38–59, <https://doi.org/10.1016/j.oregeorev.2017.12.003>
- Elmore, R.D., Dulin, S., Engel, M.H. and Parnell, J. 2006. Remagnetisation and fluid flow in the Old Red Sandstone along the Great Glen Fault, Scotland. *Journal of Geochemical Exploration*, **89**, 96–99, <https://doi.org/10.1016/j.gexplo.2005.11.034>
- Evans, K.A., Bickle, M.J., Skelton, A.D.L., Hall, M. and Chapman, H. 2002. Reductive deposition of graphite at lithological margins in East Central Vermont: a Sr, C and O isotope study. *Journal of Metamorphic Geology*, **20**, 781–798, <https://doi.org/10.1046/j.1525-1314.2002.00403.x>
- Farrell, S., Bell, K. and Clark, I. 2010. Sulphur isotopes in carbonatites and associated silicate rocks from the Superior Province, Canada. *Mineralogy and Petrology*, **98**, 209–226, <https://doi.org/10.1007/s00710-009-0101-2>
- Ferrari, A.C., Meyer, J.C. *et al.* 2006. Raman spectrum of graphene and graphene layers. *Physical Review Letters*, **97**, 187401, <https://doi.org/10.1103/PhysRevLett.97.187401>
- Ferraris, C., Groberty, B., Früh-Green, G.L. and Wessicken, R. 2004. Intergrowth of graphite within phlogopite from Finero ultramafic complex (Italian Western Alps): implications for mantle crystallisation of primary-texture mica. *European Journal of Mineralogy*, **16**, 899–908, <https://doi.org/10.1127/0935-1221/2004/0016-0899>
- Fraser, C. 1845. Parish of Kiltarlity, County of Inverness. *New Statistical Accounts of Scotland*, **XIV**, 483–502, [https://staticscot.edina.ac.uk/static/statacc/dist/viewer/nsa-vol14-Parish\\_record\\_for\\_Kiltarlity\\_in\\_the\\_county\\_of\\_Inverness\\_in\\_volume\\_14\\_of\\_account\\_2/](https://staticscot.edina.ac.uk/static/statacc/dist/viewer/nsa-vol14-Parish_record_for_Kiltarlity_in_the_county_of_Inverness_in_volume_14_of_account_2/)
- Galvez, M.E., Beyssac, O., Martinez, I., Benzerara, K., Chaduteau, C., Malvoisin, B. and Malavielle, J. 2013. Graphite formation by carbonate reduction during subduction. *Nature Geoscience*, **6**, 473–477, <https://doi.org/10.1038/NNGEO1827>
- Galvez, M.E., Fischer, W.W., Jaccard, S.L. and Eglinton, T.I. 2020. Materials and pathways of the organic carbon cycle through time. *Nature Geoscience*, **13**, 535–546, <https://doi.org/10.1038/s41561-020-0563-8>
- Garson, M.S., Coats, J.S., Rock, N.M.S. and Deans, T. 1984. Fenites, breccia dykes, albitites, and carbonatitic veins near the Great Glen Fault, Inverness, Scotland. *Journal of the Geological Society, London*, **141**, 711–732, <https://doi.org/10.1144/gsjgs.141.4.0711>
- Goldstein, R.H. and Reynolds, T.J. 1994. *Systematics of Fluid Inclusions in Diagenetic Minerals*. SEPM Short Course, **31**, <http://foldtudomany.elte.hu/fluid/fluid%20inclusions>

- Gomide, C.S., Brod, J.A. *et al.* 2013. Sulfur isotopes from alkaline carbonatite complexes. *Chemical Geology*, **341**, 38–49, <https://doi.org/10.1016/j.chemgeo.2013.01.006>
- Goodenough, K.M., Millar, I., Strachan, R.A., Krabbendam, M. and Evans, J.A. 2011. Timing of regional deformation and development of the Moine Thrust Zone in the Scottish Caledonides: constraints from the U–Pb geochronology of alkaline intrusions. *Journal of the Geological Society, London*, **168**, 99–114, <https://doi.org/10.1144/0016-76492010-020>
- Hauzenberger, C.A., Walter, F., Hofmeister, W., Phan Tien, D. and Kienzl, N. 2005. Mineralogical, petrological and crystallographic investigations of two amphiboles from ruby- and spinel-bearing marbles, Luc Yen, Province Yen Bai, Vietnam. *Berichte des Institutes für Geologie und Paläontologie der Karl-Franzens-Universität Graz*, **9**, 178–180, [https://www.zobodat.at/pdf/Ber-Inst-Erdwiss-Univ-Graz\\_9\\_0178-0180.pdf](https://www.zobodat.at/pdf/Ber-Inst-Erdwiss-Univ-Graz_9_0178-0180.pdf)
- Heptinstall, E., Parnell, J., Boyce, A.J. and Still, J. 2023. Trace element minerals from carbonatite-related fluids, The Aird, Scotland. *Scottish Journal of Geology*, **59**, <https://doi.org/10.1144/sjg2021-015>
- Home, J. and Hinxman, L.W. 1914. *Geology of Beaulieu and Inverness*. Memoir of the Geological Survey of Scotland. His Majesty's Stationery Office, Edinburgh.
- Humphreys-Williams, E. and Zahirovic, S. 2021. Carbonatites and global tectonics. *Elements*, **17**, 339–344, <https://doi.org/10.2138/gselements.17.5.339>
- Jaszczak, J.A. 1994. Famous graphite crystals from Sterling Hill, New Jersey. *The Picking Table*, **35**, 6–11, <https://pages.mtu.edu/~jaszczak/sterhill.html>
- Jaszczak, J.A. 1997. Unusual graphite crystals: from the Lime Crest Quarry, Sparta, New Jersey. *Rocks and Minerals*, **72**, 330–334, <https://doi.org/10.1080/00357529709605060>
- Jolly, W. and Cameron, J.M. 1880. On an apparently new mineral occurring in the rocks of Invernesshire. *Quarterly Journal of the Geological Society, London*, **36**, 109–111, <https://doi.org/10.1144/GSL.JGS.1880.036.01-04.11>
- Kaese, B., Kalt, A. and Pettke, T. 2007. Crystallisation and breakdown of metasomatic phases in graphite-bearing peridotite xenoliths from Marsabit (Kenya). *Journal of Petrology*, **48**, 1725–1760, <https://doi.org/10.1093/petrology/egm036>
- Kearns, L.E., Kite, L.E., Leavens, P.B. and Nelen, J.A. 1980. Fluorine distribution in the hydrous silicate minerals of the Franklin Marble. *American Mineralogist*, **65**, 557–562, [http://www.minsocam.org/ammin/AM65/AM65\\_557](http://www.minsocam.org/ammin/AM65/AM65_557)
- Kelemen, P.B. and Manning, C.E. 2015. Re-evaluating carbon fluxes in subduction zones, what goes down, mostly comes up. *Proceedings of the National Academy of Sciences of the United States of America*, **112**, E3997–E4006, <https://doi.org/10.1073/pnas.1507889112>
- Kostrovitsky, S.I., Solovjeva, L.V., Suvorova, L.Ph. and Alymova, N.V. 2001. Unusual mica peridotites and pyroxenites from Udachnaya Kimberlite, Yakutia. *Revista Brasileira de Geociências*, **31**, 505–510, <https://web.archive.org/web/20180720200715/http://ppegeo.igc.usp.br/index.php/rbg/article/download/10617/10122>
- Krabbendam, M., Strachan, R. and Prave, T. 2022. A new stratigraphic framework for the early Neoproterozoic successions of Scotland. *Journal of the Geological Society, London*, **179**, <https://doi.org/10.1144/sjg2021-054>
- Laouar, R., Boyce, A.J., Fallick, A.E. and Leake, B.E. 1990. A sulphur isotope study on selected Caledonian granites of Britain and Ireland. *Geological Journal*, **25**, 359–369, <https://doi.org/10.1002/gj.3350250318>
- Le Bas, M.J., Subbarao, K.V. and Wals, J.N. 2002. Meta-carbonatite or marble? – the case of the carbonate, pyroxenite, calcite–apatite rock complex at Borra, Eastern Ghats, India. *Journal of Asian Earth Sciences*, **20**, 127–140, [https://doi.org/10.1016/S1367-9120\(01\)00030-X](https://doi.org/10.1016/S1367-9120(01)00030-X)
- Le Breton, E., Cobbold, P.R. and Zanella, A. 2013. Cenozoic reactivation of the Great Glen Fault, Scotland: additional evidence and possible causes. *Journal of the Geological Society, London*, **170**, 403–415, <https://doi.org/10.1144/sjg2012-067>
- Leech, M.L. and Ernst, W.G. 1998. Graphite pseudomorphs after diamond? A carbon isotope and spectroscopic study of graphite cuboids from the Maksyutov Complex, south Ural Mountains, Russia. *Geochimica et Cosmochimica Acta*, **62**, 2143–2154, [https://doi.org/10.1016/S0016-7037\(98\)00142-2](https://doi.org/10.1016/S0016-7037(98)00142-2)
- Lowry, D., Boyce, A.J., Fallick, A.E., Stephens, W.E. and Grassineau, N.V. 2005. Terrane and basement discrimination in northern Britain using sulphur isotopes and mineralogy of ore deposits. *Geological Society, London, Special Publications*, **248**, 133–151, <https://doi.org/10.1144/GSL.SP.2005.248.01.07>
- Luque, F.J., Crespo-Feo, E., Barrenechea, J.F. and Ortega, L. 2012. Carbon isotopes of graphite: implications on fluid history. *Geoscience Frontiers*, **3**, 197–207, <https://doi.org/10.1016/j.gsf.2011.11.006>
- MacRae, C., Neill, I. *et al.* 2023. New U–Pb zircon data and patterns of collision magmatism in the Northern Highlands of Scotland. *EarthArXiv*, preprint, <https://eartharxiv.org/repository/view/6474/>
- Mako, C.A., Law, R.D., Caddick, M.J., Thigpen, J.R., Ashley, K.T., Cottle, J. and Kylander-Clark, A. 2019. Thermal evolution of the Scottish hinterland, Naver nappe, northern Scotland. *Journal of the Geological Society, London*, **176**, 669–688, <https://doi.org/10.1144/sjg2018-224>
- Mako, C.A., Law, R.D. *et al.* 2021. Growth and fluid-assisted alteration of accessory phases before, during and after Rodinia breakup: U–Pb geochronology from the Moine Supergroup rocks of northern Scotland. *Precambrian Research*, **355**, 106089, <https://doi.org/10.1016/j.precamres.2020.106089>
- Mendum, J.R. and Noble, S.R. 2010. Mid-Devonian sinistral transpressional movements on the Great Glen Fault: the rise of the Rosemarkie Inlier and the Acadian Event in Scotland. *Geological Society, London, Special Publications*, **335**, 161–187, <https://doi.org/10.1144/SP335.8>
- Mikhailenko, D.S., Aulbach, S. *et al.* 2021. Origin of graphite–diamond-bearing eclogites from Udachnaya kimberlite pipe. *Journal of Petrology*, **68**, egab033, <https://doi.org/10.1093/petrology/egab033>
- Milne, E.J.M., Neill, I. *et al.* 2023. Caledonian hot zone magmatism in the ‘Newer Granites’: insight from the Cluanie and Clunes plutons, Northern Scottish Highlands. *Journal of the Geological Society, London*, **180**, <https://doi.org/10.1144/sjg2022-076>
- Moro, D., Valdrè, G. *et al.* 2017. Hydrocarbons in phlogopite from Kasenyi kamafugitic rocks (SW Uganda): cross-correlated AFM, confocal microscopy and Raman imaging. *Scientific Reports*, **7**, 40663, <https://doi.org/10.1038/srep40663>
- Mykura, W. and Owens, B. 1983. *The Old Red Sandstone of the Mealfuarvonie Outlier, West of Loch Ness, Inverness-Shire*. Report of the Institute of Geological Sciences 83/7, <https://pubs.bgs.ac.uk/publications.html?pubID=B01245>
- Naemura, K., Hirajima, T. and Svojtka, M. 2009. The pressure–temperature path and the origin of phlogopite in spinel–garnet peridotites from the Blanský Les Massif of the Moldanubian Zone, Czech Republic. *Journal of Petrology*, **50**, 1795–1827, <https://doi.org/10.1093/petrology/egp052>
- Oliver, G.J.H., Wilde, S.A. and Wan, Y. 2008. Geochronology and geodynamics of Scottish granitoids from the late Neoproterozoic break-up of Rodinia to Paleozoic collision. *Journal of the Geological Society, London*, **168**, 661–674, <https://doi.org/10.1144/0016-76492007-105>
- Palache, C. 1941. Contributions to the mineralogy of Sterling Hill, New Jersey: Morphology of graphite, arsenopyrite, pyrite and arsenic. *American Mineralogist*, **26**, 709–717, [http://www.minsocam.org/ammin/AM26/AM26\\_709](http://www.minsocam.org/ammin/AM26/AM26_709)
- Parnell, J. 1985. Evidence for evaporites in the ORS of northern Scotland: replaced gypsum horizons in Easter Ross. *Scottish Journal of Geology*, **21**, 377–380, <https://doi.org/10.1144/sjg21030377>
- Parnell, J., Brolly, C. and Boyce, A.J. 2021. Mixed metamorphic and fluid graphite deposition in Palaeoproterozoic supracrustal rocks of the Lewisian Complex, NW Scotland. *Terra Nova*, **33**, 541–550, <https://doi.org/10.1111/ter.12546>
- Peach, B.N., Horne, J., Hinxman, L.W., Crampton, C.B., Anderson, E.M. and Carruthers, R.G. 1913. *The Geology of Central Ross-Shire*. Memoir of the Geological Survey of Scotland. His Majesty's Stationery Office, Edinburgh, <https://pubs.bgs.ac.uk/publications.html?pubID=B01955>
- Peck, W.H., Volkert, R.A., Meredith, M.T. and Rader, E.L. 2006. Calcite–graphite thermometry of the Franklin marble, New Jersey Highlands. *The Journal of Geology*, **114**, 485–499, <https://doi.org/10.1086/504181>
- Rajesh, V., Arai, S. and Satish-Kumar, M. 2009. Origin of graphite in glimmerite and spinelite in Achankovil Shear Zone, southern India. *Journal of Mineralogical and Petrological Sciences*, **104**, 407–412, <https://doi.org/10.2465/jmps.090622d>
- Rathbone, P.A. and Harris, A.L. 1980. Moine and Lewisian near the Great Glen Fault in Easter Ross. *Scottish Journal of Geology*, **16**, 51–64, <https://doi.org/10.1144/sjg16010051>
- Rock, N.M.S., Jeffreys, L.A. and MacDonal, R. 1984. The problem of anomalous local limestone–pelite successions within the Moine outcrop; 1: metamorphic limestones of the Great Glen area, from Ardgour to Nigg. *Scottish Journal of Geology*, **20**, 383–406, <https://doi.org/10.1144/sjg20030383>
- Rock, N.M.S., Macdonald, R., Drewery, S.E., Pankhurst, R.J. and Brook, M. 1986a. Pelites of the Glen Urquhart serpentinite–metamorphic complex, west of Loch Ness (Anomalous local limestone–pelite successions within the Moine outcrop: III). *Scottish Journal of Geology*, **22**, 179–202, <https://doi.org/10.1144/sjg22020179>
- Rock, N.M.S., Macdonald, R., Szucs, T. and Bower, J. 1986b. The comparative geochemistry of some Highland pelites (anomalous local limestone–pelite successions within the Moine outcrop: II). *Scottish Journal of Geology*, **22**, 107–126, <https://doi.org/10.1144/sjg22010107>
- Rock, N.M.S., Davis, A.E., Hutchinson, D., Joseph, M. and Smith, T.K. 1987. The geochemistry of Lewisian marbles. *Geological Society, London, Special Publications*, **27**, 109–126, <https://doi.org/10.1144/GSL.SP.1987.027.01.10>
- Rogers, G. and Dunning, G.R. 1991. Geochronology of appinitic and related granitic magmatism in the W Highlands of Scotland: constraints on the timing of transcurrent fault movement. *Journal of the Geological Society, London*, **148**, 17–27, <https://doi.org/10.1144/gsjgs.148.1.0017>
- Rumble, D., Duke, E.F. and Hoering, T.L. 1986. Hydrothermal graphite in New Hampshire: evidence of carbon mobility during regional metamorphism. *Geology*, **14**, 452–455, [https://doi.org/10.1130/0091-7613\(1986\)14<452:HGHNHE>2.0.CO;2](https://doi.org/10.1130/0091-7613(1986)14<452:HGHNHE>2.0.CO;2)
- Satish-Kumar, M. 2005. Graphite-bearing CO<sub>2</sub>–fluid inclusions in granulites: Insights on graphite precipitation and carbon isotope evolution. *Geochimica et Cosmochimica Acta*, **69**, 3841–3856, <https://doi.org/10.1016/j.gca.2005.02.007>
- Satish-Kumar, M. and Niimi, N. 1998. Fluorine-rich clinohumite from Ambasamudram marbles, Southern India: mineralogical and preliminary FTIR spectroscopic characterization. *Mineralogical Magazine*, **62**, 509–519, <https://doi.org/10.1180/002646198547882>

- Satish-Kumar, M. and Wada, H. 1997. Meteoric water infiltration in Skallen marbles, East Antarctica: oxygen isotopic evidence. *Proceedings of the NIPR Symposium on Antarctic Geosciences*, **10**, 111–119.
- Satish-Kumar, M. and Wada, H. 2000. Carbon isotope equilibrium between calcite and graphite in Skallen Marbles, East Antarctica: evidence for the preservation of peak metamorphic temperatures. *Chemical Geology*, **166**, 173–182, [https://doi.org/10.1016/S0009-2541\(99\)00189-8](https://doi.org/10.1016/S0009-2541(99)00189-8)
- Satish-Kumar, M., Jaszczak, J.A., Hamamatsu, T. and Wada, H. 2011. Relationship between structure, morphology, and carbon isotopic composition of graphite in marbles: Implications for calcite-graphite carbon isotope thermometry. *American Mineralogist*, **96**, 470–485, <https://doi.org/10.2138/am.2011.3576>
- Satish-Kumar, M., Shirakawa, M. *et al.* 2021. A geochemical and isotopic perspective on tectonic setting and depositional environment of Precambrian meta-carbonate rocks in collisional orogenic belts. *Gondwana Research*, **96**, 163–204, <https://doi.org/10.1016/j.gr.2021.03.013>
- Schito, A., Romano, C., Corrado, S., Grigo, D. and Poe, B. 2017. Diagenetic thermal evolution of organic matter by Raman spectroscopy. *Organic Geochemistry*, **106**, 57–67, <https://doi.org/10.1016/j.orggeochem.2016.12.006>
- Searle, M.P. 2022. Tectonic evolution of the Caledonian orogeny in Scotland: a review based on the timing of magmatism, metamorphism and deformation. *Geological Magazine*, **159**, 124–152, <https://doi.org/10.1017/S0016756821000947>
- Shields, G. and Veizer, J. 2002. Precambrian marine carbonate isotope database: Version 1.1. *Geochemistry, Geophysics, Geosystems*, **3**, <https://doi.org/10.1029/2001GC000266>
- Stewart, M., Strachan, R.A. and Holdsworth, R.E. 1999. Structure and early kinematic history of the Great Glen Fault zone, Scotland. *Tectonics*, **18**, 326–342, <https://doi.org/10.1029/1998TC900033>
- Stewart, M., Strachan, R.A., Martin, M.W. and Holdsworth, R.E. 2001. Constraints on early sinistral displacement along the Great Glen Fault Zone, Scotland: structural setting, U–Pb geochronology and emplacement of the syn-tectonic Clunes tonalite. *Journal of the Geological Society, London*, **158**, 821–830, <https://doi.org/10.1144/jgs.158.5.821>
- Strachan, R.A. and Evans, J.A. 2008. Structural setting and U–Pb zircon geochronology of the Glen Scaddle Metagabbro: evidence for polyphase Scandian ductile deformation in the Caledonides of northern Scotland. *Geological Magazine*, **145**, 361–371, <https://doi.org/10.1017/S0016756808004500>
- Strachan, R.A., Holdsworth, R.E., Krabbendam, M. and Alsop, G.I. 2010. The Moine Supergroup of NW Scotland: insights into the analysis of polyorogenic supracrustal sequences. *Geological Society, London, Special Publications*, **335**, 233–254, <https://doi.org/10.1144/SP335.11>
- Strachan, R.A., Alsop, G.I., Ramezani, J., Frazer, R.E., Burns, I.M. and Holdsworth, R.E. 2020a. Patterns of Silurian deformation and magmatism during sinistral oblique convergence, northern Scottish Caledonides. *Journal of the Geological Society, London*, **177**, 893–910, <https://doi.org/10.1144/jgs2020-039>
- Strachan, R.A., Johnson, T.E., Kirkland, C.L., Kinny, P.D. and Kusky, T. 2020b. A Baltic heritage in Scotland: Basement terrane transfer during the Glenvillian orogeny. *Geology*, **48**, 1094–1098, <https://doi.org/10.1130/G47615.1>
- Sun, J., Yang, Y., Ingrin, J., Wang, Z. and Xia, Q. 2022. Impact of fluorine on the thermal stability of phlogopite. *American Mineralogist*, **107**, 815–825, <https://doi.org/10.2138/am-2022-8051>
- Sutton, J. and Watson, J. 1951. The supposed Lewisian inlier of Scardroy, central Ross-shire, and its relations with the surrounding Moine rocks. *Quarterly Journal of the Geological Society, London*, **108**, 99–126, <https://doi.org/10.1144/GSL.JGS.1952.108.01-04.05>
- Tamas, A., Holdsworth, R.E. *et al.* 2023. Older than you think: using U–Pb calcite geochronology to better constrain basin-bounding fault reactivation, Inner Moray Firth Basin, western North Sea. *Journal of the Geological Society, London*, **180**, <https://doi.org/10.1144/jgs2022-166>
- Underhill, J.R. and Brodie, J.A. 1993. Structural geology of Easter Ross, Scotland: implications for movement on the Great Glen Fault zone. *Journal of the Geological Society, London*, **150**, 515–527, <https://doi.org/10.1144/gsjgs.150.3.0515>
- Wada, H., Tomita, T., Matsuura, K., Tuchi, K., Ito, M. and Morikiyo, T. 1994. Graphitisation of carbonaceous matter during metamorphism with references to carbonate and pelitic rocks of contact and regional metamorphisms, Japan. *Contributions to Mineralogy and Petrology*, **118**, 217–228, <https://doi.org/10.1007/BF00306643>
- Wallace, T. 1885. Notes on northern minerals. *Mineralogical Magazine*, **6**, 168–170, <https://doi.org/10.1180/minmag.1885.006.030.05>
- Wallace, T.D. 1887. Geology of the Parish of Kirkhill and the ‘Aird’, Inverness-shire. *Transactions of the Edinburgh Geological Society*, **5**, 224–234, <https://doi.org/10.1144/transed.5.2.224>
- Walters, A.S., Goodenough, K.M., Hughes, H.S.R., Roberts, N.M.W., Gunn, A.G., Rushton, J. and Lacinska, A. 2013. Enrichment of Rare Earth Elements during magmatic and post-magmatic processes: a case study from the Loch Loyal Syenite Complex, northern Scotland. *Contributions to Mineralogy and Petrology*, **166**, 1177–1202, <https://doi.org/10.1007/s00410-013-0916-z>
- Wopenka, B. and Pasteris, J.D. 1993. Structural characterization of kerogen to granulite-facies graphite: Applicability of Raman microprobe spectroscopy. *American Mineralogist*, **78**, 533–557, [http://www.minsocam.org/ammin/AM78/AM78\\_533](http://www.minsocam.org/ammin/AM78/AM78_533)
- Wright, A.J., Blamey, N.J.F., Conliffe, J., Costanzo, A. and Parnell, J. 2012. Origin of vein-graphite derived from metamorphic fluids in Moine (Glenfinnan Group) rocks, NW Scotland. *Scottish Journal of Geology*, **48**, 47–59, <https://doi.org/10.1144/0036-9276/01-426>
- Wu, C. 2008. Bayan Obo controversy: carbonatites versus iron oxide–Cu–Au–(REE–U). *Resource Geology*, **58**, 348–354, <https://doi.org/10.1111/j.1751-3928.2008.00069.x>
- Yang, T., Sun, X., Shi, G., Li, D. and Zhou, H. 2019. The genetic linkage between the Yuanjiang marble-hosted ruby deposit and Cenozoic tectonic evolution of the Ailao Shan–Red River shear zone (Southwest China). *Journal of Asian Earth Sciences*, **177**, 38–47, <https://doi.org/10.1016/j.jseas.2019.03.010>